present study might be a reason for the lack of severe hypoglycemic episodes.

Progression of retinopathy was observed in three patients. Aggressive reduction of BG levels in patients with long-term poor glycemic control has been reported to be a factor contributing to early retinopathy progression after glycemic control[29–31] and a slow reduction rate of HbA_{1c} levels (slower than −0.5% per month) is recommended for such patients[32]. The patient in the present study who withdrew because of marked retinopathy progression had a long-term poor glycemic state; longer insulin titration intervals than those used in the present study might be desirable for such patients. However, progression of retinopathy was reported in another two patients, whose baseline HbA_{1c} levels and reduction rates were not as high and not as aggressive, respectively (from 7.8 to 6.9% and from 7.2 to 6.3% during 6 months), indicating that the fast reduction rate of HbA_{1c} levels is only a definitive cause of early retinopathy worsening after aggressive glycemic control. Although causes for retinopathy progression in our patients are not clear, patients who undergo intensified glycemic control regimens should be followed up with careful and regular observation of retinopathy to prevent or to take an appropriate action against its worsening.

The present study was limited by low numbers of patients. Accordingly, the aforementioned results must be interpreted as those of a limited pilot study. A large number of participants is necessary to conclude that the regimen of the present study is a suitable method for the initiation of insulin therapy in Japanese T2D patients.

In summary, an addition of a once-daily pre-dinner injection of BIAsp 30 using a patient-directed insulin titration method on the basis of SMBG levels according to a predetermined algorithm can provide satisfactory reduction of HbA_{1c} levels and flat BG profiles from post-dinner to pre-breakfast in Japanese T2D patients with failure of OAD therapies. Lower post-breakfast BG excursions at baseline, shorter diabetes duration and younger age might warrant optimal glycemic control, including daytime postprandial BG profiles, with safety after this simple insulin initiating regimen.

ACKNOWLEDGEMENT

The authors declare no conflict of interest.

REFERENCES

1. The Diabetes Control and Complications Trial Research Group. The effect of intensive treatment of diabetes on the development and progression of long-term complications of insulin-dependent diabetes mellitus. *N Engl J Med* 1993; 329: 977–986.
2. Ohkubo Y, Kishikawa H, Araki E, *et al.* Intensive insulin therapy prevents the progression of diabetic microvascular complications in Japanese patients with non-insulin-dependent diabetes mellitus: a randomized prospective 6-year study. *Diabetes Res Clin Pract* 1995; 28: 103–117.
3. UK Prospective Diabetes Study (UKPDS) Group. Intensive blood-glucose control with sulphonylureas or insulin compared with conventional treatment and risk of complications in patients with type 2 diabetes (UKPDS 33). *Lancet* 1998; 352: 837–853.
4. Holman RR, Paul S, Bethel MA, *et al.* 10-year follow-up of intensive glucose control in type 2 diabetes. *N Engl J Med*, 2008; 359: 1577–1589.
5. Japan Diabetes Society. *Treatment Guide for Diabetes*. Tokyo: Bunkodo, 2007.
6. Nathan DM, Buse JB, Davidson MB, *et al.* Medical management of hyperglycemia in type 2 diabetes: a consensus algorithm for the initiation and adjustment of therapy: a consensus statement of the American Diabetes Association and the European Association for the Study of Diabetes. *Diabetes Care* 2009; 32: 193–203.
7. UK Prospective Diabetes Study Group. UK Prospective Diabetes Study 16: overview of 6 year's therapy of type 2 diabetes: a progressive disease. *Diabetes* 1995; 44: 1249–1258.
8. Kahn SE, Haffner SM, Heise MA, *et al.* Glycemic durability of rosiglitazone, metformin, or glyburide monotherpay. *N Engl J Med* 2006; 355: 2427–2443.
9. Riddle MC, Rosenstock J, Gerich J, *et al.* The treat-to-target trial: randomized addition of glargine or human NPH insulin to oral therapy of type 2 diabetic patients. *Diabetes Care* 2003; 26: 3080–3086.
10. Eliaschewitz FG, Calvo C, Valbuena H, *et al.* Therapy in type 2 diabetes: insulin glargine vs. NPH insulin both in combination with glimepiride. *Arch Med Res* 2006; 37: 495–501.
11. Hermansen K, Davies M, Derezinski T, *et al.* A 26-week, randomized, parallel, treat-to-target trial comparing insulin detemir with NPH insulin as add-on therapy to oral glucose-lowering drugs in insulin-naïve people with type 2 diabetes. *Diabetes Care* 2006; 29: 1269–1274.
12. Philis-Tsimikas A, Charpentier G, Clauson P, *et al.* Comparison of once-daily insulin detemir with NPH insulin added to a regimen of oral antidiabetic drugs in poorly controlled type 2 diabetes. *Clin Ther* 2006; 28: 1569–1581.
13. Yki-Järvinen H, Kauppinen-Mäkelin R, Tiikkainen M, *et al.* Insulin glargine or NPH combined with metformin in type 2 diabetes: the LANMET study. *Diabetologia* 2006; 49: 442–451.
14. Rosenstock J, Davies M, Home PD, *et al.* A randomised, 52-week, treat-to-target trial comparing insulin detemir with insulin glargine when administered as add-on to glucose-lowering drugs in insulin-naive people with type 2 diabetes. *Diabetologia* 2008; 51: 408–416.
15. Goto H, Hirose T, Shimizu T, *et al.* Effectiveness of combination therapy with a sulfonylurea and once-daily insulin glargine in Japanese type 2 diabetic patients. Evaluation of the long-term (18 months) results of the combination therapy. *J Japan Diab Soc* 2007; 50: 591–597.
16. Hermansen K, Colombo M, Storgaard H, *et al.* Improved postprandial glycemic control with biphasic insulin aspart relative to biphasic insulin lispro and biphasic human insulin

in patients with type 2 diabetes. *Diabetes Care* 2002; 25: 883–888.
17. McSorley PT, Bell PM, Jacobsen LV, *et al.* Twice-daily biphasic insulin aspart 30 versus biphasic human insulin 30: a double-blind crossover study in adults with type 2 diabetes mellitus. *Clin Ther* 2002; 24: 530–539.
18. Garber AJ, Wahlen J, Wahl T, *et al.* Attainment of glycaemic goals in type 2 diabetes with once-, twice-, or thrice-daily dosing with biphasic insulin aspart 70/30 (The 1-2-3 study). *Diabetes Obes Metab* 2006; 8: 58–66.
19. Yoshioka N, Kurihara Y, Manda N, *et al.* Step-up therapy with biphasic insulin aspart-70/30; -Sapporo 1-2-3 study. *Diabetes Res Clin Pract* 2009; 85: 47–52.
20. Strojek K, Bebakar WMW, Khutsoane DT, *et al.* Once-daily initiation with biphasic insulin aspart 30 versus insulin glargine in patients with type 2 diabetes inadequately controlled with oral drugs: an open-label, multinational RCT. *Curr Med Res Opin* 2009; 25: 2887–2894.
21. Davies M, Storms F, Shutler S, *et al.* Improvement of glycemic control in subjects with poorly controlled type 2 diabetes. Comparison of two treatment algorithms using insulin glargine. *Diabetes Care* 2005; 28: 1282–1288.
22. Meneghini L, Koenen C, Weng W, *et al.* The usage of a simplified self-titration dosing guideline (303 Algorithm) for insulin detemir in patients with type 2 diabetes. Results of the randomized, controlled PREDICTIVE 303 study. *Diabetes Obes Metab* 2007; 9: 902–913.
23. Kosaka K, Hagura R, Kuzuya T. Insulin responses in equivocal and definite diabetes, with special reference to subjects who had mild glucose intolerance but later developed definite diabetes. *Diabetes* 1977; 26: 944–952.
24. Mitsui R, Fukushima M, Nishi Y, *et al.* Factors responsible for deteriorating glucose tolerance in newly diagnosed type 2 diabetes in Japanese men. *Metabolism* 2006; 55: 53–58.
25. Jensen CC, Cnop M, Hull RL, *et al.* B-Cell Function is a major contributor to oral glucose tolerance in high-risk relatives of four ethnic groups in the US. *Diabetes* 2002; 51: 2170–2178.
26. Kadowaki T, Miyake Y, Hagura R, *et al.* Risk factors for worsening to diabetes in subjects with impaired glucose tolerance. *Diabetologia* 1984; 26: 44–49.
27. Yoshiuchi K, Matsuhisa M, Katakami N, *et al.* Glycated albumin is a better indicator for glucose excursion than glycated hemoglobin in type 1 and type 2 diabetes. *Endocr J* 2008; 55: 503–507.
28. Kashiwagi A, Kadowaki T, Haneda M, *et al.* Consensus and statement on international standardization of HbA1C in Japan: committee report on diabetes mellitus laboratory testing standardization. *J Japan Diab Soc* 2009; 52: 811–818.
29. Daneman D, Drash A, Lobes LA, *et al.* Progressive retinopathy with improved control in diabetic dwarfism (Mauriac's syndrome). *Diabetes Care* 1981; 4: 360–365.
30. Morita C, Hasumi S, Omori Y, *et al.* Effects of the rapid control of blood glucose to the diabetic retinopathy; from the aspect of the internist. *Diabetes Journal* 1992; 20: 7–12.
31. The Diabetes Control and Complications Trial Research Group. Early worsening of diabetic retinopathy in the diabetes control and complications trial. *Arch Ophthalmol* 1998; 116: 874–886.
32. Shichiri M. Glycemic control and diabetic retinopathy. *Folia Ophthalmol Jpn* 1996; 47: 1–6.

Biochemical and Biophysical Research Communications 404 (2011) 115–120

Contents lists available at ScienceDirect

Biochemical and Biophysical Research Communications

journal homepage: www.elsevier.com/locate/ybbrc

The effect of gastric inhibitory polypeptide on intestinal glucose absorption and intestinal motility in mice

Eiichi Ogawa [a], Masaya Hosokawa [a,b], Norio Harada [a], Shunsuke Yamane [a], Akihiro Hamasaki [a], Kentaro Toyoda [a], Shimpei Fujimoto [a], Yoshihito Fujita [a], Kazuhito Fukuda [a], Katsushi Tsukiyama [a,c], Yuichiro Yamada [a,c], Yutaka Seino [a,d], Nobuya Inagaki [a,e,*]

[a] Department of Diabetes and Clinical Nutrition, Graduate School of Medicine, Kyoto University, Japan
[b] Faculty of Human Sciences, Tezukayama Gakuin University, Osaka, Japan
[c] Department of Internal Medicine, Division of Endocrinology, Diabetes and Geriatric Medicine, Akita University School of Medicine, Akita, Japan
[d] Kansai Electric Power Hospital, Osaka, Japan
[e] CREST of Japan Science and Technology Cooperation (JST), Kyoto, Japan

ARTICLE INFO

Article history:
Received 21 October 2010
Available online 21 November 2010

Keywords:
GIP
Glucose absorption
Intestine

ABSTRACT

Gastric inhibitory polypeptide (GIP) is released from the small intestine upon meal ingestion and increases insulin secretion from pancreatic β cells. Although the GIP receptor is known to be expressed in small intestine, the effects of GIP in small intestine are not fully understood. This study was designed to clarify the effect of GIP on intestinal glucose absorption and intestinal motility. Intestinal glucose absorption *in vivo* was measured by single-pass perfusion method. Incorporation of [^{14}C]-glucose into everted jejunal rings *in vitro* was used to evaluate the effect of GIP on sodium-glucose co-transporter (SGLT). Motility of small intestine was measured by intestinal transit after oral administration of a non-absorbed marker. Intraperitoneal administration of GIP inhibited glucose absorption in wild-type mice in a concentration-dependent manner, showing maximum decrease at the dosage of 50 nmol/kg body weight. In glucagon-like-peptide-1 (GLP-1) receptor-deficient mice, GIP inhibited glucose absorption as in wild-type mice. *In vitro* examination of [^{14}C]-glucose uptake revealed that 100 nM GIP did not change SGLT-dependent glucose uptake in wild-type mice. After intraperitoneal administration of GIP (50 nmol/kg body weight), small intestinal transit was inhibited to 40% in both wild-type and GLP-1 receptor-deficient mice. Furthermore, a somatostatin receptor antagonist, cyclosomatostatin, reduced the inhibitory effect of GIP on both intestinal transit and glucose absorption in wild-type mice. These results demonstrate that exogenous GIP inhibits intestinal glucose absorption by reducing intestinal motility through a somatostatin-mediated pathway rather than through a GLP-1-mediated pathway.

1. Introduction

Gastric inhibitory polypeptide (GIP), also called glucose-dependent insulinotropic polypeptide, is an incretin of 42-amino-acid polypeptide synthesized by K cells of the duodenum and small intestine [1]. We previously generated GIP receptor-deficient mice (GIPR$^{-/-}$ mice) and showed that GIPR$^{-/-}$ mice have higher blood glucose levels as well as impaired initial insulin response after oral glucose load [2]. Thus, early insulin secretion stimulated by GIP plays an important role in glucose tolerance after oral glucose load.

While GIP receptor mRNA was reported to be present in rat gut [3], the role of the GIP receptor in the gut has not been fully clarified. In this *in vivo* study, we investigated the effect of exogenous GIP on intestinal glucose absorption in mice using the intestinal perfusion method. We investigated the effect of exogenous GIP on SGLT-dependent glucose uptake *in vitro* by using the everted jejunal ring method. Because intestinal motility and absorption are positively related [4,5], we investigated the effect of exogenous GIP on gastrointestinal motility by non-absorbed marker method. Since SST secretion has been reported to be stimulated by GIP and to prolong intestinal motility, we also investigated the involvement of SST in the inhibitory effect of exogenous GIP on both intestinal transit and intestinal glucose absorption by using somatostatin receptor antagonist. Our results demonstrate that exogenous GIP inhibits intestinal glucose absorption by reducing intestinal motility through a somatostatin-mediated pathway rather than through a GLP-1-mediated pathway.

Abbreviations: GIP, Gastric inhibitory polypeptide; GLP-1, glucagon-like-peptide-1; SST, somatostatin; SGLT, sodium-glucose co-transporter; CSS, cyclosomatostatin.

* Corresponding author. Address: Department of Diabetes and Clinical Nutrition, Graduate School of Medicine, Kyoto University, 54 Shogoin, Kawahara-cho, Sakyo-ku, Kyoto 606-8507, Japan. Fax: +81 75 771 6601.
E-mail address: inagaki@metab.kuhp.kyoto-u.ac.jp (N. Inagaki).

0006-291X/$ - see front matter © 2010 Elsevier Inc. All rights reserved.
doi:10.1016/j.bbrc.2010.11.077

2. Materials and methods

2.1. Animals

Male C57/BL6J mice weighing 25–30 g (8–14 weeks old) were housed in a temperature (25 ± 2 °C)- and moisture (50%)-controlled room with a 12 h light/dark cycle (6:00 AM/6:00 PM). The mice were fed standard mouse chow (Oriental Yeast, Osaka) and tap water *ad libitium*, and used as wild-type mice.

Generation of GIPR$^{-/-}$ mice and GLP-1 receptor-deficient mice (GLP-1R$^{-/-}$ mice) was described previously [2,6]. GLP-1R$^{-/-}$ mice were kindly provided by Dr. Daniel J. Drucker [6]. Age-matched male GIPR$^{-/-}$ and GLP-1R$^{-/-}$ mice were used in the experiments. The Animal Care Committee of Kyoto University Graduate School of Medicine approved animal care and procedures.

2.2. Materials

Synthetic human GIP was purchased from Peptide Institute (Osaka, Japan). The somatostatin receptor antagonist, cyclo(7-aminoheptanoyl-PHE-D-TRP-LYS-THR(BZL)) (cyclosomatostatin (CSS)) and somatostatin 28 (SST) were from Sigma Chemical Co. (St. Louis, MO). All other chemicals were of reagent grade.

2.3. Perfusion experiment

Single-pass perfusion method [7] was used to measure the effect of exogenous GIP or SST on intestinal glucose absorption using C57/BL6J mice. Preperfusion was done for a 45 min equilibration period and the samples were discarded. Three 15 min samples were then collected. GIP or SST was administered intraperitoneally at 60 min after starting the preperfusion according to the protocol (Fig. 1A). The change of absorption was calculated as the glucose concentration of the first sample collected (Period 1) minus the glucose concentration of the last sample collected (Period 2), and expressed as per centimeter perfused bowel. Negative values indicate an inhibitory effect on absorption; positive values indicate an increased effect on absorption.

2.4. Glucose uptake in jejunum in vitro

Incorporation of D-glucose into everted jejunal rings was determined as described previously [8]. SGLT-dependent glucose uptake for 15 min was determined as the glucose uptake in the absence of phlorizin minus the glucose uptake in the presence of phlorizin.

2.5. Small intestinal transit after intraperitoneal administration of GIP

Transit through the stomach and small intestine was measured by administering a non-absorbed marker containing 10% charcoal suspension in 5% gum Arabic, as previously described [9]. The mice were given 0.2 ml of the suspension by gavage through a straight blunt-ended feeding needle. GIP (50 nmol/kg body weight) or SST (75 nmol/kg body weight) or vehicle (saline) was administered intraperitoneally 15 min prior to the administration of the non-absorbed marker. CSS (1 μg/kg body weight), or vehicle (saline) was intraperitoneally administered 10 min prior to GIP administration.

2.6. Plasma GIP and SST assays

Blood was collected from the tail vein before the intraperitoneal administration of GIP (50 nmol/kg body weight) and collected again 20 min after the administration. ELISA assay kit was used according to the manufacture's instruction for the determination of plasma total GIP concentration (Linco Research, St. Charles, MO) and SST concentration (Phoenix Pharmaceuticals INC., Belmont, CA), respectively.

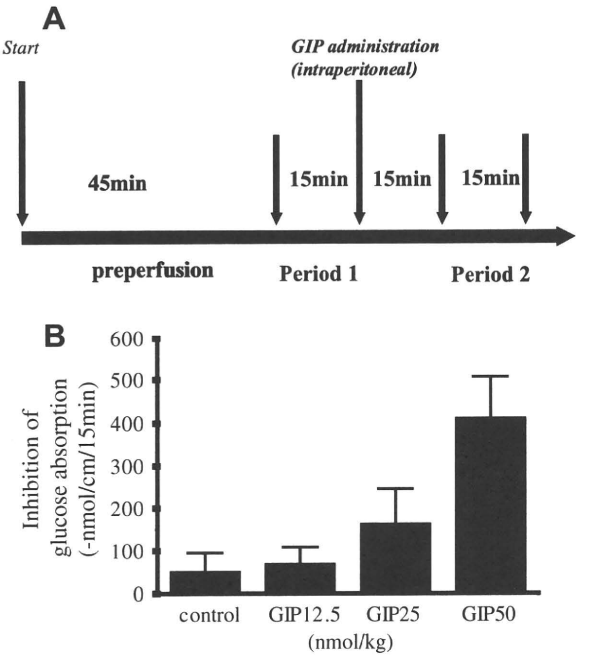

Fig. 1. (A) Diagram showing the sampling protocol of intestinal perfusion. The flow rate of the perfusion fluid was 2 ml/15 min. Perfusion began with an equilibration period of 45 min, which samples were discarded. The samples of Period 1 and Period 2 were then collected. GIP was administered intraperitoneally 60 min after the beginning of preperfusion. The change of absorption was calculated as the glucose concentration of the first samples collected (Period 1) minus the glucose concentration of the last samples collected (Period 2), and expressed as per centimeter perfused bowel. (B) Concentration-dependence of inhibition of glucose absorption by GIP in wild-type mice. Data are shown as means with SEM ($n = 6$ for each group, $P < 0.05$ by ANOVA).

2.7. Analysis

The results are given as mean ± standard error (SEM, n = number of mice). Statistical significance was determined using paired and unpaired Student's t-test and analysis of variance (ANOVA). $P < 0.05$ was considered significant.

3. Results

3.1. Perfusion experiment

Inhibition of glucose absorption was calculated by change in glucose concentration in effluent perfusate in wild-type mice (Fig. 1A). Spontaneous inhibition of glucose absorption of 49 ± 44 nmol/cm/15 min is shown in saline-administered controls (Fig. 1B). Inhibition of glucose absorption was enhanced to 67 ± 40, 163 ± 84, and 409 ± 96 nmol/cm/15 min when the amount of intraperitoneally-administered GIP was increased to 12.5, 25, and 50 nmol/kg body weight, respectively.

3.2. Glucose uptake by jejunum in vitro

We investigated glucose uptake by the jejunum *in vitro* using everted jejunal rings. In the presence of 100 nM GIP in the incubation medium, glucose uptake into jejunal rings in wild-type mice was similar to that in the presence of vehicle (control: 4.2 ± 0.9 μmol/g weight; GIP: 3.5 ± 0.9, P = NS; Fig. 2A). Additionally, glucose uptake into jejunal rings in GIPR$^{-/-}$ mice was similar

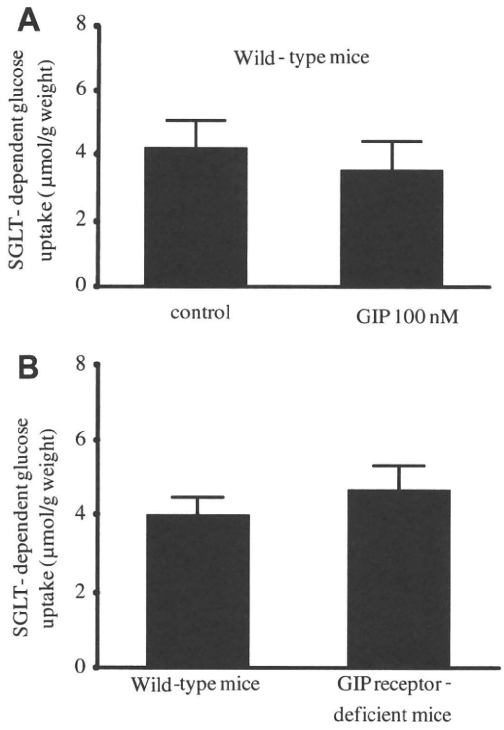

Fig. 2. Glucose uptake in the jejunum. (A) Glucose uptake in the jejunum in wild-type mice in the absence and in the presence of 100 nM GIP. (B) Glucose uptake in the jejunum in wild-type and GIPR$^{-/-}$ mice. SGLT-dependent glucose uptake was determined as the glucose uptake in the absence of 1 mM phlorizin minus the glucose uptake in the presence of 1 mM phlorizin. Data are shown as means with SEM (n = 8 for each group).

to that in wild-type mice (wild-type mice: 4.0 ± 0.5 μmol/g weight; GIPR$^{-/-}$ mice 4.6 ± 0.7, P = NS; Fig. 2B).

3.3. Small intestinal transit after intraperitoneal administration of GIP

Intestinal transit rate was measured by the length of small intestine traversed by the charcoal suspension. In wild-type mice, the intestinal transit rate in GIP-administered mice was significantly less than that in saline-administered control (45 ± 8% vs. 68 ± 4%, $P < 0.01$; Fig. 3A). On the other hand, in GIPR$^{-/-}$ mice, the intestinal transit rate was similar to that in saline-administered control and GIP-administered mice (65 ± 3% vs. 63 ± 4%; Fig. 3B).

3.4. Perfusion and intestinal transit in GLP-1 receptor-deficient mice

To determine whether GIP affects intestinal glucose absorption through GLP-1 signaling, inhibition of glucose absorption by GIP was measured in GLP-1R$^{-/-}$ mice. Inhibition of glucose absorption in GLP-1R$^{-/-}$ mice was 44 ± 100 nmol/cm/15 min in saline-administered control mice and 426 ± 104 nmol/cm/15 min in GIP-administered mice (50 nmol/kg body weight, $P < 0.05$, Fig. 3C). Thus, GIP significantly inhibited glucose absorption in GLP-1R$^{-/-}$ mice.

The intestinal transit rate was also evaluated in GLP-1R$^{-/-}$ mice, and was 59 ± 13% in saline-administered control and 42 ± 7% in GIP-administered mice, respectively. Thus, GIP significantly inhibited the intestinal transit rate in GLP-1R$^{-/-}$ mice ($P < 0.01$, Fig. 3D). Consequently, the genetic disruption of GLP-1 receptor did not affect GIP action on intestinal glucose absorption and intestinal transit.

3.5. Involvement of SST in the action of GIP

To determine whether the inhibitory effect of GIP on intestinal transit is due to release of SST, a somatostatin receptor antagonist, CSS (1 μg/kg body weight), was intraperitoneally administered 10 min prior to GIP administration in wild-type mice (Fig. 4A). In the presence of CSS, the intestinal transit rate in GIP-administered wild-type mice was significantly higher than that in the absence of CSS (60 ± 3% vs. 45 ± 8%; $P < 0.01$). Accordingly, CSS reduced the inhibitory effect of GIP on intestinal transit. Moreover, intraperitoneally-administered SST itself significantly inhibited the intestinal transit rate in wild-type mice compared to control (SST: 37 ± 5% vs. control: 68 ± 4%, $P \leqslant 0.01$).

In a perfusion experiment, to confirm that the inhibitory effect of GIP on intestinal glucose absorption is attributable to release of SST, CSS (1 μg/kg body weight) was intraperitoneally administered 10 min prior to GIP administration in wild-type mice (Fig. 4B). In

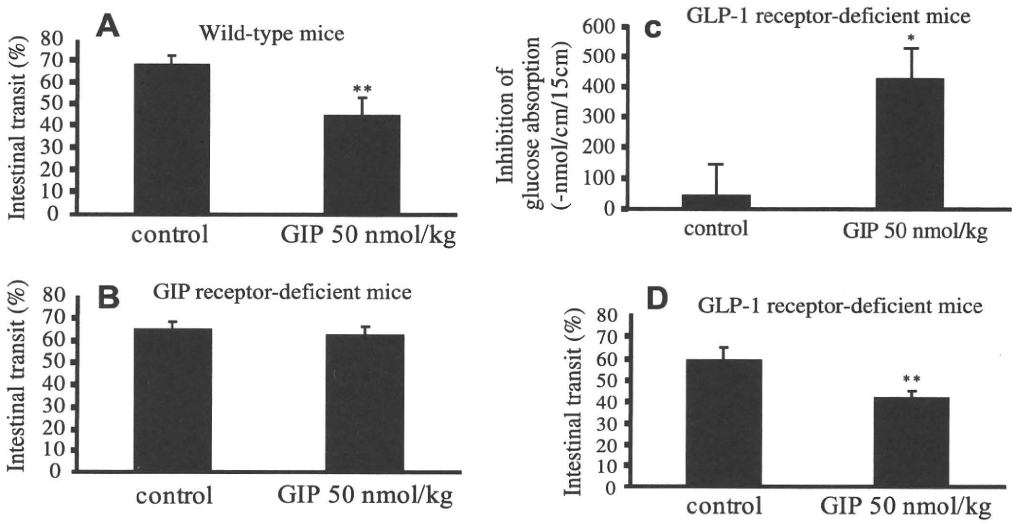

Fig. 3. Intestinal transit after oral administration of non-absorbed marker (10% charcoal suspension in 5% gum Arabic) in wild-type (A) and GIPR$^{-/-}$ (B) mice. Twenty minutes after administration of non-absorbed marker by gavage, the animals were killed and the entire gastrointestinal transit tract was removed. GIP (50 nmol/kg body weight) or saline was administered intraperitoneally 15 min prior to the administration of non-absorbed marker. Data are shown as means with SEM (n = 6 for each group). Statistical significance was determined using Student's t-test. **$P < 0.01$ compared with control. (C) Inhibition of glucose absorption in GLP-1R$^{-/-}$ mice with or without intraperitoneal GIP administration as indicated in the legends of Fig 1. (D) Intestinal transit after oral administration of non-absorbed marker in GLP-1R$^{-/-}$ mice with or without intraperitoneal GIP administration as indicated in the legends of Fig 3A. Data are shown as means with SEM (n = 6 for each group). Statistical significance was determined using Student's t-test. *$P < 0.05$ compared with control.

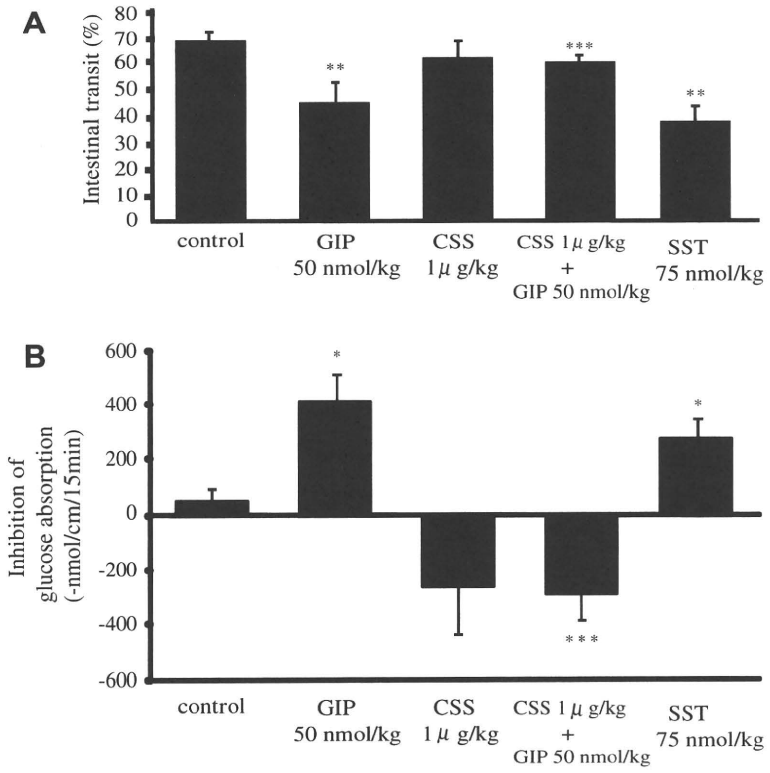

Fig. 4. (A) Intestinal transit after oral administration of non-absorbed marker in wild-type mice with or without pretreatment of CSS. The rate of transit was determined as indicated in the legend of Fig 3A. GIP or SST or saline was administered intraperitoneally 15 min prior to the administration of non-absorbed marker. CSS or saline was intraperitoneally administered 10 min prior to GIP administration. Data are shown as means with SEM ($n = 6$ for each group). Statistical significance was determined using Student's t-test. $^{**}P < 0.01$ compared with control. $^{***}P < 0.01$ compared with GIP alone administered mice. (B) Inhibition of glucose absorption by GIP in wild-type mice with or without pretreatment of CSS, and inhibition of glucose absorption by SST. CSS or saline was intraperitoneally administered 10 min prior to GIP administration. Data are shown as means with SEM ($n = 6$ for each group). Statistical significance was determined using Student's t-test. $^{*}P < 0.05$ compared with control. $^{***}P < 0.01$ compared with GIP alone administered mice.

the presence of CSS, the inhibition of glucose absorption in GIP-administered wild-type mice was significantly lower than that in the absence of CSS (410 ± 96 nmol/cm/15 min vs. −290 ± 99 nmol/cm/15 min; $P < 0.01$). Accordingly, CSS reduced the inhibitory effect of GIP on intestinal glucose absorption. Furthermore, inhibition of glucose absorption in wild-type mice was 49 ± 44 nmol/cm/15 min in saline-administered control mice and 278 ± 63 nmol/cm/15 min in SST-administered mice (75 nmol/kg body weight, $P < 0.05$).

In an experiment of glucose uptake in everted jejunal ring, 100 nM SST did not alter glucose uptake compared to control (control: 4.2 ± 0.9 μmol/g weight; SST: 4.2 ± 0.4, $n = 8$; P = NS).

3.6. Measurement of plasma GIP and SST levels

The plasma levels of total GIP and SST in mice were significantly enhanced 20 min after the intraperitoneal GIP-administration at a dosage of 50 nmol/kg body weight compared to the respective basal levels (GIP: 58 ± 5 pg/ml vs. 3400 ± 257 pg/ml, $n = 8$; $P < 0.01$; SST: 9.9 ± 0.5 ng/ml vs.11.9 ± 0.3 ng/ml, $n = 8$; $P < 0.05$).

4. Discussion

We investigated the inhibitory effect of exogenous GIP on glucose absorption in small intestine. GIP has been known as an important insulinotropic hormone released from duodenal K cells. However, there have been few reports on the effects of GIP on intestinal glucose absorption. In this study, GIP was found to inhibit glucose absorption in a concentration-dependent manner by the perfusion method.

Glucose absorption includes two steps in enterocytes, permeation through brush-border membrane and subsequently through basolateral membrane. Glucose and galactose cross the brush-border membrane by means of SGLT-1, which is a rate-limiting step of glucose absorption [10]. Recent *in vitro* study by Singh et al. found that exogenous GIP stimulates SGLT-dependent glucose absorption by using an Ussing chamber experiment [11]. In the experiment, intestine was fixed between two chambers, and short-circuit-current representing SGLT activity was measured. However, in our experiments using everted jejunal rings, which is another method to measure SGLT-dependent glucose absorption *in vitro*, the lack of effect of exogenous GIP on SGLT-dependent glucose uptake was shown, and genetic disruption of the GIP receptor was found not to affect SGLT-dependent glucose absorption. The reason why our results and theirs are different is unknown, but may be attributable to difference in method.

It is generally accepted that there is a positive relationship between intestinal motility and absorption [4,5]. It has been shown that increased intestinal motility, besides enhancing the functional surface area, facilitates diffusion of glucose to the transporters of the brush-border membrane by altering the unstirred water layer [12,13]. We investigated the effect of GIP on motility of small intestine by evaluating intestinal transit. In this study, GIP was found to inhibit intestinal transit compared to control in wild-type but not in $GIPR^{-/-}$ mice. Thus, the inhibitory effect of GIP on glucose absorption may be attributable, in part, to inhibition of intestinal motility.

GLP-1, another incretin hormone, is secreted from L cells found predominantly in ileal mucosa, and is known to be part of the "ileal brake" that acts as an inhibitor of upper gastrointestinal motility

[14]. In this study, GIP was found to inhibit intestinal transit in GLP-1R$^{-/-}$ mice as well as in wild-type mice, indicating that the inhibitory action of GIP on gastrointestinal transit is not mediated by GLP-1. Furthermore, glucose absorption was found to be inhibited significantly by GIP in GLP-1R$^{-/-}$ mice as well as in wild-type mice, suggesting that the primary mechanism of the inhibition of intestinal glucose absorption by GIP most likely does not involve the GLP-1-mediated pathway.

Recently, Miki et al. reported that GLP-1 inhibited gut motility while GIP did not [15]. In this study, however, GIP was found to inhibit intestinal transit. The inconsistency could be due to their use of a non-absorbed marker containing a high concentration (as much as 50%) of glucose to evaluate gut motility, whereas we used a non-absorbed marker without glucose. Intraduodenal infusion of hyperosmolar solution was reported to increase duodenal motility, which is mediated by activation of osmoreceptors in duodenum [16]. In our preliminary experiment on small intestinal transit using 10% charcoal suspension in 5% gum Arabic with 50% glucose, the intestinal transit rate was significantly greater than that when using glucose-free solution (88 ± 8% vs. 68 ± 4%, $P < 0.05$, unpublished data). Therefore, intestinal transit might be enhanced by the high concentration of glucose itself in the suspension, which could conceal a GIP-evoked inhibitory effect on intestinal transit. However, limitations of this study must be considered. While GIP was found to inhibit intestinal transit under the conditions of this study, the effect of GIP on intestinal transit may differ among the constituents of the food or nutrient. Further investigations are required.

Regarding the GIP dosage applied in the *in vivo* experiments, low GIP dosage has been used when applied by the route of continuous intravenous administration; GIP (0.25 nmol/kg body weight) was reported to stimulate insulin secretion by intravenous administration in rat [17] and (GIP 4 pmol/kg body weight/min) in human [18]. However, high GIP dosage has been used when applied by the other routes of administration than intravenous administration. Indeed, one group has reported that subcutaneous pre-administration of 100 μg GIP (approximately 800 nmol/kg body weight) lowered glucose excursion in oral glucose tolerance test in mice [15] and another group has reported that intraperitoneal administration of [D-Ala^2]GIP (48 nmol/kg body weight/day), a DPP4-resistant analogue, lowered glucose excursion in intraperitoneal glucose tolerance test in mice [19]. In this study, we applied GIP intraperitoneally at a dosage of 50 nmol/kg body weight to demonstrate the pharmacological effects of GIP on intestinal transit and glucose absorption, which dosage is comparable to those used in the latter reports.

Regarding the mechanism of inhibition of intestinal transit by GIP, SST secretion has been reported to be stimulated by GIP [20–22] and to prolong intestinal transit [23,24]. The SST receptor has five isoforms (sst1-5) and all five receptors have been shown to be expressed in gastrointestinal tract, with high levels of sst2 receptor in intestine [25]. The sst2 receptors in intestine have been shown not to be expressed on enterocytes or muscle cells, but on myenteric and submucosal plexuses and on neuroendocrine cells in epithelium [26] and also on interstitial cells of Cajal in deep muscular plexus [27]. Thus, the mechanisms by which exogenous GIP inhibits intestinal motility through two SST-mediated pathways may be as follows. In the first, exogenous GIP binds to the GIP receptors on the cell surface membrane in SST-containing enteric neurons and/or in mucosal endocrine cells of D cells in gastrointestinal tract and/or in pancreatic islets, resulting in the release of SST. Subsequently, the released SST acts as a neurotransmitter and binds to sst2 receptors expressed on other neurons in myenteric plexus, parts of which nerve fibers are distributed to muscular cells, permitting inhibition of intestinal motility. In this pathway, the local SST concentration in interneural synaptic space may be increased prominently. In an alternate pathway, SST secreted from D cells flows into systemic circulation through submucosal vessels to reach the neurons in myenteric plexus. Indeed, in this study, intraperitoneally-administered GIP induced a small but significant increase in plasma SST levels, suggesting involvement of the latter pathway.

In our experiment of intestinal perfusion, GIP was found to inhibit intestinal glucose absorption primarily by reducing intestinal motility. On the other hand, the tissue of everted intestinal ring is set inside-out and distended far from the physiological condition, and thus incapable of reflecting general intestinal motility. Thus, the lack of GIP action on glucose uptake in the tissues of everted intestinal ring in this study may be expected.

Several studies have found that the inhibitory effect of SST on intestinal glucose absorption may be attributable to either the effect of SST on the splanchnic hemodynamics [28] or a direct effect of SST on enterocytes [29]. However, consistent with this study, another study has found that SST delays intestinal glucose absorption by its inhibitory effect on intestinal motility [24]. SST exerts its inhibitory effect on intestinal glucose absorption by several mechanisms; our results indicate that the inhibitory effect of SST is mediated, at least in part, by alteration of intestinal motility.

In this study, the somatostatin receptor antagonist CSS was found to reduce the inhibitory effect of GIP on intestinal transit, suggesting that GIP stimulates SST release. In addition, we show that SST itself inhibits intestinal transit and glucose absorption in perfused intestine. Consistently, a recent study has reported that SST inhibits intestinal glucose absorption [29]. Considered together with previous reports, we conclude that exogenous GIP inhibits intestinal transit and glucose absorption indirectly through a somatostatin-mediated pathway.

One of the physiological roles of GIP is known to be facilitation of nutrient uptake into adipose tissue and bone. In this study, exogenous GIP was found to inhibit intestinal glucose absorption by reducing intestinal motility. Since this observation was obtained by the action of a supraphysiological level of plasma GIP, it is unclear whether or not the action is associated with already known physiological actions of GIP. In the point of delay of intestinal carbohydrate absorption, however, the biological action of GIP found in this study appears to be similar to that of medical medicine α-glucosidase inhibitor, which does not influence the regulation of energy accumulation in adipose tissue or bone.

Acknowledgments

This study was supported by Scientific Research Grants and a Grant for Leading Project for Biosimulation from the Ministry of Education, Culture, Sports, Science, and Technology of Japan, a grant from CREST of Japan Science and Technology Cooperation, and a grant from the Ministry of Health, Labor, and Welfare, Japan, and also by Kyoto University Global COE Program "Center for Frontier Medicine". The authors are grateful to Dr. Daniel J. Drucker for kindly providing GLP-1R$^{-/-}$ mice.

References

[1] Y. Seino, M. Fukushima, D. Yabe, GIP and GLP-1, the two incretin hormones: similarities and differences, J. Diabetes Invest. 1 (2010) 8–23.
[2] K. Miyawaki, Y. Yamada, H. Yano H, et al., Glucose intolerance caused by a defect in the entero-insular axis: a study in gastric inhibitory polypeptide receptor knockout mice, Proc. Natl. Acad. Sci. USA 96 (1999) 14843–14847.
[3] T.B. Usdin, E. Mezey, D.C. Button, et al., Gastric inhibitory polypeptide receptor, a member of the secretin-vasoactive intestinal peptide receptor family, is widely distributed in peripheral organs and the brain, Endocrinology 133 (1993) 2861–2870.
[4] M. Sababi, U.H. Bengtsson, Enhanced intestinal motility influences absorption in anaesthetized rat, Acta Physiol. Scand. 172 (2001) 115–122.
[5] A.J. Smout, Small intestinal motility, Curr. Opin. Gastroenterol. 20 (2004) 77–81.

[6] L.A. Scrocchi, T.J. Brown, N. MaClusky, et al., Glucose intolerance but normal satiety in mice with a null mutation in the glucagon-like peptide 1 receptor gene, Nat. Med. 2 (1996) 1254–1258.
[7] R. Athman, A. Tsocas, O. Presset, et al., In vivo absorption of water and electrolytes in mouse intestin, Application to villin$^{-/-}$ mice, Am. J. Physiol. Gastrointest. Liver Physiol. 282 (2002) G634–639.
[8] K. Tsukiyama, Y. Yamada, K. Miyawaki, et al., Gastric inhibitory polypeptide is the major insulinotropic factor in K(ATP) null mice, Eur. J. Endocrinol. 151 (2004) 407–412.
[9] K. Yamada, M. Hosokawa, S. Fujimoto, et al., The spontaneously diabetic Torii rat with gastroenteropathy, Diabetes Res. Clin. Pract. 75 (2007) 127–134.
[10] M.A. Hediger, M.J. Coady, T.S. Ikeda, et al., Expression cloning and cDNA sequencing of the Na^+/glucose co-transporter, Nature 330 (1987) 379–381.
[11] S.K. Singh, A.C. Bartoo, S. Krishnan, et al., Glucose-dependent insulinotropic polypeptide (GIP) stimulates transepithelial glucose transport, Obesity 16 (2008) 2412–2416.
[12] F.A. Wilson, J.M. Dietschy, The intestinal unstirred layer: its surface area and effect on active transport kinetics, Biochim. Biophys. Acta 363 (1974) 112–126.
[13] D.V. Rayner, The relationships between glucose absorption and insulin secretion and the migrating myoelectric complex in the pig, Exp. Physiol. 76 (1991) 67–76.
[14] A. Wettergren, B. Schjoldager, P.E. Mortensen, et al., Truncated GLP-1 (proglucagon 78–107-amido) inhibits gastric and pancreatic functions in man, Dig. Dis. Sci. 38 (1993) 665–673.
[15] T. Miki, K. Minami, H. Shinozaki, et al., Distinct effects of glucose-dependent insulinotropic polypeptide and glucagon-like peptide-1 on insulin secretion and gut motility, Diabetes 54 (2005) 1956–1963.
[16] H.C. Lin, J.D. Elashoff, G.M. Kwok, et al., Stimulation of duodenal motility by hyperosmolar mannitol depends on local osmoreceptor control, Am. J. Physiol. 266 (1994) G940–943.
[17] E.L. Mazzaferri, L. Ciofalo, L.A. Waters, et al., Effects of gastric inhibitory polypeptide on leucine- and arginine-stimulated insulin release, Am. J. Physiol. 245 (1983) E114–E120.
[18] T. Vilsbøll, T. Krarup, S. Madsbad, et al., Defective amplification of the late phase insulin response to glucose by GIP in obese Type II diabetic patients, Diabetologia 45 (2002) 1111–1119.
[19] B.J. Lamont, D.J. Drucker, Differential antidiabetic efficacy of incretin agonists versus DPP-4 inhibition in high fat fed mice, Diabetes 57 (2008) 190–198.
[20] J. Szecówka, V. Grill, E. Sandberg, et al., Effect of GIP on the secretion of insulin and somatostatin and the accumulation of cyclic AMP in vitro in the rat, Acta Endocrinol. (Copenh) 99 (1982) 416–421.
[21] L. Hansen, J.J. Holst, The effects of duodenal peptides on glucagon-like peptide-1 secretion from the ileum. A duodeno–ileal loop?, Regul Pept. 110 (2002) 39–45.
[22] J.J. Holst, S.L. Jensen, S. Knuhtsen, et al., Effect of vagus, gastric inhibitory polypeptide, and HCl on gastrin and somatostatin release from perfused pig antrum, Am. J. Physiol. 244 (1983) G515–522.
[23] G.J. Krejs, Effect of somatostatin and absorption and atropine infusion on intestinal transit tine and fructose absorption in the perfused human jejunum, Diabetes 33 (1984) 548–551.
[24] C. Johansson, O. Wisén, S. Efendić, et al., Effects of somatostatin on gastrointestinal propagation and absorption of oral glucose in man, Digestion 22 (1981) 126–137.
[25] K. Krempels, B. Hunyady, A.M. O'Carroll, et al., Distribution of somatostatin receptor messenger RNAs in the rat gastrointestinal tract, Gastroenterology 112 (1997) 1948–1960.
[26] M. Gugger, B. Waser, A. Kappeler, et al., Cellular detection of sst2A receptors in human gastrointestinal tissue, Gut 53 (2004) 1431–1436.
[27] C. Sternini, H. Wong, S.V. Wu, et al., Somatostatin 2A receptor is expressed by enteric neurons, and by interstitial cells of Cajal and enterochromaffin-like cells of the gastrointestinal tract, J. Comp. Neurol. 386 (1997) 396–408.
[28] J. Wahren, Influence of somatostatin on carbohydrate disposal and absorption in diabetes mellitus, Lancet 2 (1976) 1213–1216.
[29] F. Féry, L. Tappy, P. Schneiter, et al., Effect of somatostatin on duodenal glucose absorption in man, J. Clin. Endocrinol. Metab. 90 (2005) 4163–4169.

Exendin-4 Protects Pancreatic Beta Cells from the Cytotoxic Effect of Rapamycin by Inhibiting JNK and p38 Phosphorylation

Authors: Y. Kawasaki[1], S. Harashima[1], M. Sasaki[1], E. Mukai[1,2], Y. Nakamura[1], N. Harada[1], K. Toyoda[1], A. Hamasaki[1], S. Yamane[1], C. Yamada[1], Y. Yamada[1,3], Y. Seino[1,4], N. Inagaki[1,5]

Affiliations: Affiliation addresses are listed at the end of the article

Key words
- exendin-4
- rapamycin
- JNK
- p38
- beta cells

Abstract

It has been reported that the immunosuppressant rapamycin decreases the viability of pancreatic beta cells. In contrast, exendin-4, an analogue of glucagon-like peptide-1, has been found to inhibit beta cell death and to increase beta cell mass. We investigated the effects of exendin-4 on the cytotoxic effect of rapamycin in beta cells. Incubation with 10 nM rapamycin induced cell death in 12 h in murine beta cell line MIN6 cells and Wistar rat islets, but not when coincubated with 10 nM exendin-4. Rapamycin was found to increase phosphorylation of c-Jun amino-terminal kinase (JNK) and p38 in 30 minutes in MIN6 cells and Wistar rat islets while exendin-4 decreased their phosphorylation. Akt and extracellular signal-regulated kinase (ERK) were not involved in the cytoprotective effect of exendin-4. These results indicate that exendin-4 may exert its protective effect against rapamycin-induced cell death in pancreatic beta cells by inhibiting JNK and p38 signaling.

received 19.09.2009
accepted 08.02.2010

Bibliography
DOI http://dx.doi.org/10.1055/s-0030-1249035
Published online: March 8, 2010
Horm Metab Res 2010; 42: 311–317

ISSN 0018-5043

Correspondence
N. Inagaki, MD, PhD
Department of Diabetes and Clinical Nutrition
Graduate School of Medicine
Kyoto University
54 Shogoin Kawahara-cho
Sakyo-ku
606-8507 Kyoto
Japan
Tel.: +81/75/751 3560
Fax: +81/75/771 6601
inagaki@metab.kuhp.kyoto-u.ac.jp

Introduction

Exendin-4 is presently being used in patients with type 2 diabetes [1]. The glucagon-like peptide-1 (GLP-1) analogue improves blood glucose levels by increasing insulin secretion. Exendin-4 is also suggested to promote beta cell proliferation and neogenesis and to inhibit beta cell apoptosis, thereby increasing beta cell mass, at least in rodents [2]. Apoptosis induced by inflammatory cytokines [3] or endoplasmic reticulum (ER) stress [4] was shown to be prevented by exendin-4 in primary rat beta cells and INS-1, a murine beta cell line. Treatment with exendin-4 markedly attenuates beta cell apoptosis in db/db mice [5] and in male C57BL/6 mice exposed to streptozotocin [6]. The molecular mechanism of the cytoprotective effect of exendin-4 is mediated by increased levels of cyclic AMP (cAMP) that lead to activation of protein kinase A (PKA), enhanced insulin receptor substrate-2 (IRS-2) activity, and activation of Akt and extracellular signal-regulated kinase (ERK) [7]. Recently it was reported that exendin-4 inhibits cytokine-induced apoptosis, which involves electron transport chain proteins of mitochondria with a reduction of oxidative stress in INS-1 cells [8].

Rapamycin, an immunosuppressant used to prevent rejection in organ transplantation, is reported to impair glucose-stimulated insulin secretion in rat islets and to decrease viability of rat and human islets [9]. A recent study suggested that rapamycin reduces beta cell mass by 50% under diabetic conditions in *Psammomys obesus*, an animal model of nutrition-dependent type 2 diabetes, by increasing c-Jun amino-terminal kinase (JNK) phosphorylation [10].

We investigated whether exendin-4 might ameliorate the cytotoxic effects of rapamycin. In the present study, we found that rapamycin induces cell death in beta cells through an increase in phosphorylation of JNK and p38, and that exendin-4 prevents such rapamycin-induced cell death by inhibiting these molecules.

Materials and Methods

Materials

Tissue culture media, DMEM and RPMI1640, rapamycin, exendin-4, exendin (9–39) (exendin-9), H89, LY294002, PD98059, SP600125, SB203580, RNaseA, propidium iodide (PI), and anti-α-tubulin antibody (Ab) were obtained from Sigma Aldrich (St Louis, MO, USA). Fetal bovine

serum (FBS) was from Invitrogen (Carlsbad, CA, USA). Anti-phospho-Akt (Ser473) Ab, anti-Akt Ab, anti-phospho-JNK (Thr183/Tyr185) Ab, anti-JNK Ab, anti-phospho-p38 (Thr180/Tyr182) Ab, anti-p38 Ab, anti-caspase-3 Ab, and anti-cleaved caspase-3 Ab were obtained from Cell Signaling (Danvers, MA, USA). Anti-phospho-ERK Ab and anti-ERK Ab were from Santa Cruz Biotechnology (Santa Cruz, CA, USA).

Methods

Cell culture and stimulation of MIN6 cells

MIN6 cells were maintained in 25 mM glucose DMEM media supplemented with 13% FBS, 100 U/ml penicillin, 100 µg/ml streptomycin, and 5 µl β-mercaptoethanol at 37 °C in humidified air containing 5% CO_2. For the experiment, the cells (1.2×10^6) were plated into 35 mm dishes, incubated in DMEM media with or without protein kinase inhibitors for 30 min, and rapamycin and/or exendin-4, and/or forskolin, and/or exendin-9 were then added into the media. After the indicated time periods, the cells were collected and analyzed for cell death and protein phosphorylation.

Islet isolation and stimulation

Pancreatic islets were isolated from Wistar rats by collagenase digestion as described previously [11], and preincubated in RPMI 1640 medium containing 10% FBS, 100 U/ml penicillin, 100 µg/ml streptomycin, and 5.5 mM glucose at 37 °C in humidified air containing 5% CO_2 for 60 min. After preincubation, the islets were cultured in the media with 10 nM rapamycin and/or 10 nM exendin-4 for the indicated time periods and then analyzed for cell death, protein phosphorylation, and insulin secretion and content.

Insulin secretion and content

Insulin secretion from islets was monitored using batch incubation as previously described [11]. After islets were cultured with 10 nM rapamycin and/or 10 nM exendin-4 for 12 h, the islets were collected, washed, and preincubated at 37 °C for 30 min in Krebs-Ringer bicarbonate buffer (KRBB) medium supplemented with 2.8 mM glucose, and groups of 5 islets were then batch-incubated for 30 min in 0.7 ml KRBB medium containing 2.8 mM and 16.7 mM glucose. At the end of the incubation period, the islets were pelleted by centrifugation, and aliquots of the buffer were sampled to determine the amount of immunoreactive

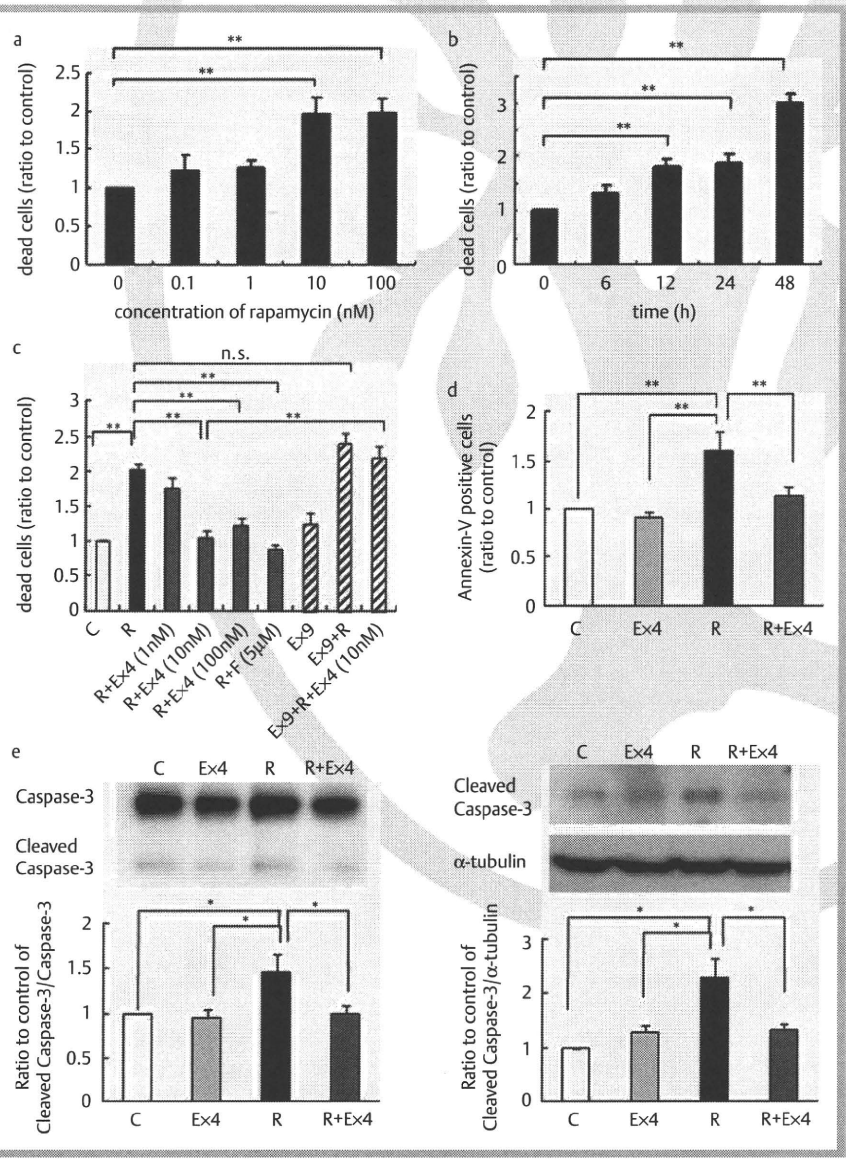

Fig. 1 Exendin-4 inhibits rapamycin-induced cell death in MIN6 cells. **a**: Dose-dependency and **b**: time-dependency of rapamycin-induced cell death in MIN6 cells. MIN6 cells were treated with 0.1, 1, 10, or 100 nM rapamycin for 12 h (**a**) or with 10 nM rapamycin for 6, 12, 24, or 48 h (**b**), and dead cells with sub-G1 DNA content were counted by flowcytometer. Data are means ± SE of five independent experiments. ** $p < 0.01$. **c**: Quantification of dead cells 12 h after treatment with DMSO (control), 10 nM rapamycin, 10 nM rapamycin and 1, 10, or 100 nM exendin-4, 10 nM rapamycin and 5 µM forskolin, 100 nM exendin-9, and 100 nM exendin-9 and 10 nM rapamycin with or without 10 nM exendin-4. Data are means ± SE of four independent experiments. ** $p < 0.01$. **d**: The percentage of annexin-V-FITC positive cells. MIN6 cells were cultured with 10 nM rapamycin and/or 10 nM exendin-4, and annexin-V-FITC positive cells were counted by flowcytometer. Data are means ± SE of three independent experiments. ** $p < 0.01$. **e**: Western blot analysis of caspase-3 and cleaved caspase-3 in MIN6 cells treated with 10 nM rapamycin and/or 10 nM exendin-4 for 12 h. Images are representative of three independent experiments. Graphs show relative ratio of cleaved caspase-3 versus caspase-3 or α-tubulin, respectively. * $p < 0.05$. C: control (DMSO); R: rapamycin; Ex4: exendin-4; F: forskolin; Ex9: exendin-9.

insulin by RIA. After an aliquot of incubation medium for insulin release assay in 2.8 mM glucose was taken, the remaining islets were lysed and insulin contents were determined.

Quantification of cell death

MIN6 cells incubated under the conditions indicated were collected from both attached and floating cell populations and fixed with 70% ethanol for 4 h. The cells were then washed with PBS, incubated in phosphate-citrate buffer for 30 min, resuspended in 10 µg/ml RNaseA containing PBS, and stained with 10 µg/ml PI. Dead cells containing sub-G1 DNA content were identified and analyzed by a FACS Calibur instrument (BD Biosciences, San Jose, CA, USA). Annexin-V positive cells were analyzed by FACS Calibur using annexin-V-FITC Apoptosis Detection Kit (BD Pharmingen, San Diego, CA, USA). Primary islets were cultured in the indicated conditions for 12 h. DNA fragmentation was measured by quantification of cytosolic oligonucleosome-bound DNA using Cell Death Detection ELISA (Roche, Mannheim, Germany) as previously described [12]. To detect caspase-3 activity, MIN6 cells and primary islets were cultured with 10 nM rapamycin and/or 10 nM exendin-4 for 12 h, and 50 µg of the proteins were subjected to western blot analysis.

Western blot analysis

Cells were collected and washed twice with PBS, and then sonicated in lysis buffer. Equivalent amounts of protein were resolved by SDS/PAGE on 4–12% acrylamide gels (Invitrogen) and transferred to PVDF membranes (Invitrogen), followed by immunoblotting with antibodies to detect respective proteins.

Fluorescence labeling with Newport Green

Islet beta cells from Wistar rat were cultured with 10 nM rapamycin and/or 10 nM exendin-4 for 12 h and stained with Newport Green (Invitrogen) for 30 min. The labeled beta cells were visualized by fluorescence microscopy (Keyence, New Jersey, USA).

Statistics

Data are expressed as mean ± SE. Statistical comparisons were made between groups using one-way analysis of variance. Significant differences were evaluated using Tukey-Kramer post hoc analysis.

Results

Exendin-4 inhibits rapamycin-induced cell death in MIN6 cells

We first examined the dose-dependency and time-dependency of rapamycin-induced cell death in MIN6 cells. The number of dead cells was significantly increased in 10 and 100 nM rapamycin-treated MIN6 cells compared to that in DMSO-treated cells (control) in 12 h (◎ **Fig. 1a**). The number of dead cells induced by 10 nM rapamycin, a therapeutic concentration in blood [13], was significantly increased from 12 h and maximized at 48 h (◎ **Fig. 1b**), indicating cytotoxicity in MIN6 cells in 12 h.

MIN6 cells were then treated with 1, 10, or 100 nM exendin-4 in the presence of 10 nM rapamycin for 12 h. The number of rapamycin-induced dead cells was significantly reduced by 97.0 ± 14.9% and 78.1 ± 14.5% by coincubation with 10 and 100 nM exendin-4, respectively (◎ **Fig. 1c**). In addition, 5 µM forskolin, an adenylyl cyclase activator, completely blocked rapamycin-induced cell death (◎ **Fig. 1c**). In addition, exendin-9, an

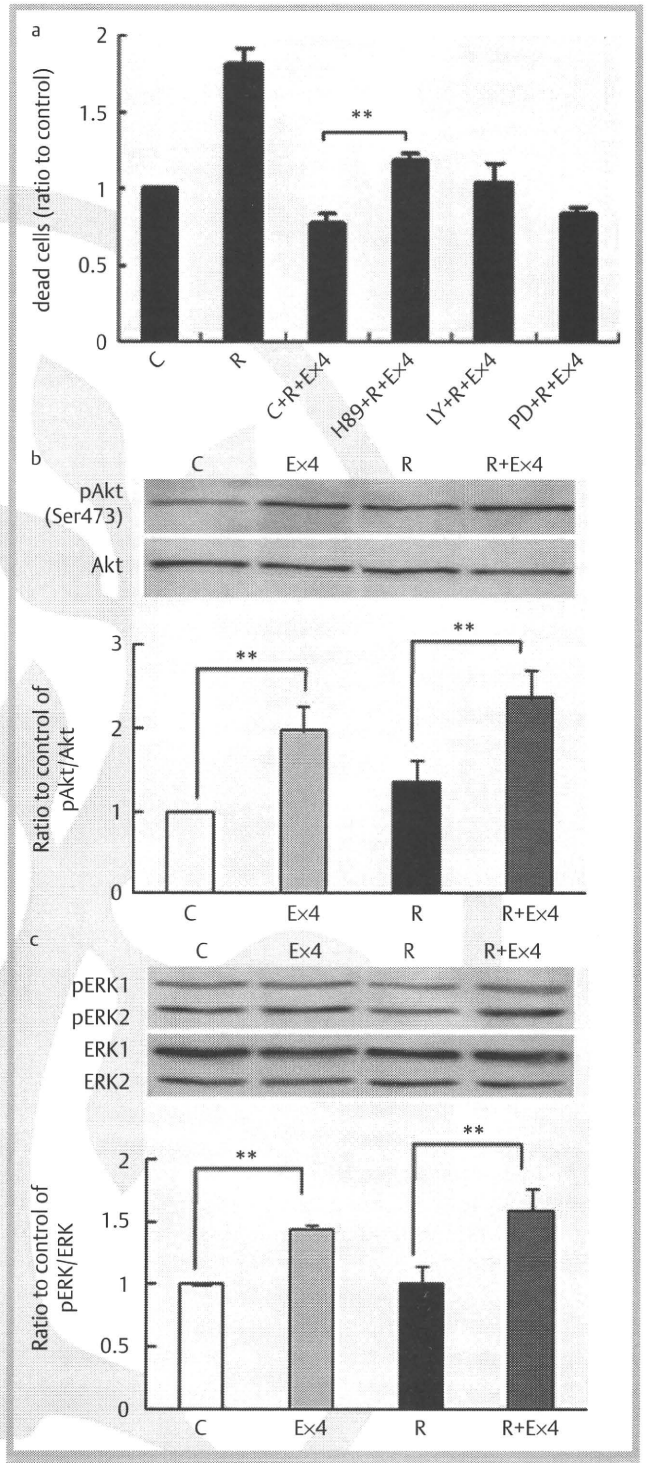

Fig. 2 Cytoprotective effect of exendin-4 is partially mediated by PKA, but not by PI3K/Akt and ERK. **a**: The percentage of dead cells with sub-G1 DNA content. DMSO (control), 15 µM H89, 10 µM LY294002, or 50 µM PD98059 was added into the media 30 min before treatment with 10 nM rapamycin and 10 nM exendin-4 for 12 h in MIN6 cells, and dead cells were counted by flowcytometer. Data are means ± SE of four independent experiments. ** $p<0.01$. **b**, **c**: Western blot analysis of Akt and ERK in MIN6 cells treated with 10 nM rapamycin and/or 10 nM exendin-4 for 30 min. Images are representative of three independent experiments. Graphs show relative ratio of phosphorylated Akt or ERK vs. total Akt or ERK, respectively, by treatment with rapamycin and/or exendin-4 compared to control (DMSO). Data are means ± SE of three independent experiments. ** $p<0.01$. C: control (DMSO); R: rapamycin; Ex4: exendin-4; LY: LY294002; PD: PD98059.

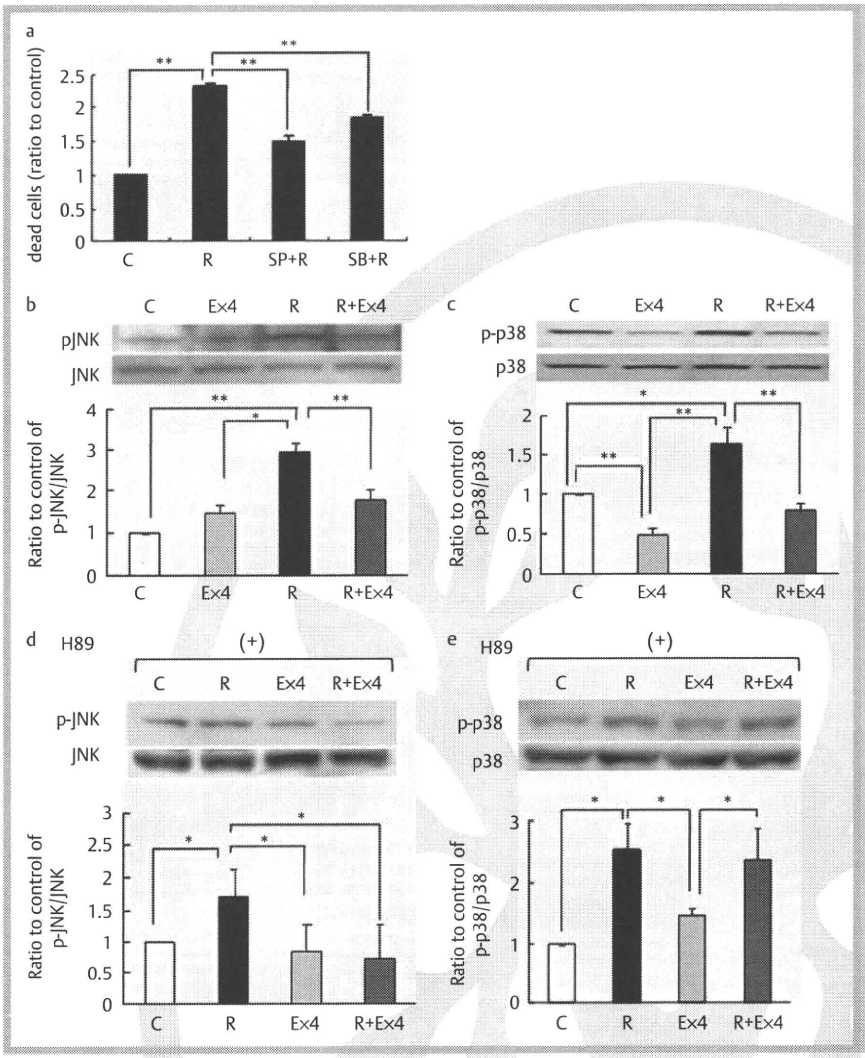

Fig. 3 Exendin-4 inhibits rapamycin-induced cell death by decreasing JNK and p38 phosphorylation in MIN6 cells. **a**: The percentage of dead cells with sub-G1 DNA content. DMSO (control), 10 µM SP600125 or 10 µM SB203580 was added into MIN6 cells 30 min before treatment with 10 nM rapamycin for 12 h, and dead cells were counted by flowcytometer. Data are means ± SE of four independent experiments. ** $p<0.01$.
b, **c**: Western blot analysis of JNK and p38 in MIN6 cells treated with 10 nM rapamycin and/or 10 nM exendin-4 for 30 min. **d**, **e**: Western blot analysis of JNK and p38 in MIN6 cells to which 15 µM H89 was added 30 min before incubation with 10 nM rapamycin and/or 10 nM exendin-4 for 30 min. Images are representative of three independent experiments. Graphs show relative ratio of phosphorylated JNK or p38 v.s. total JNK or p38, respectively, by treatment with rapamycin and/or exendin-4 compared to control (DMSO). Data are means ± SE of three independent experiments. * $p<0.05$ ** $p<0.01$. C: control (DMSO); R: rapamycin; Ex4: exendin-4; SP: SP600125; SB: SB203580.

antagonist of the GLP-1 receptor, inhibited the cytoprotective effect of exendin-4 on rapamycin-induced cell death (◎ **Fig. 1c**). Annexin-V-positive apoptotic cells were also significantly increased in rapamycin-treated MIN6 cells compared to those in control cells, which increase was prevented by treatment with exendin-4 (◎ **Fig. 1d**). Furthermore, rapamycin increased caspase-3 activity, while exendin-4 decreased it in rapamycin-treated MIN6 cells (◎ **Fig. 1e**). These results indicate that exendin-4 inhibits rapamycin-induced cell death through the GLP-1 receptor by an increase in the intracellular cAMP concentration in MIN6 cells.

Cytoprotective effect of exendin-4 is mediated in part by PKA, but not by PI3K and ERK

We then examined the involvement of PKA, phosphatidylinositol 3-kinase (PI3K)/Akt, and ERK, downstream molecules of the GLP-1 receptor signaling pathways. DMSO (control), 15 µM H89, a PKA inhibitor, 10 µM LY294002, a PI3K inhibitor, or 50 µM PD98059, an ERK inhibitor, was added into the media 30 min before treatment with 10 nM exendin-4 and 10 nM rapamycin for 12 h in MIN6 cells, and dead cells were counted by flowcytometer. H89, a PKA inhibitor, partially but significantly blocked the cytoprotective effect of exendin-4 (◎ **Fig. 2a**). On the other hand, neither LY294002 nor PD98059 altered the cytoprotective effect of exendin-4 against rapamycin-induced cell death (◎ **Fig. 2a**), although phosphorylation of Akt and ERK was significantly increased by treatment with exendin-4 (◎ **Fig. 2b** and **c**). These results indicate that PKA is involved, at least in part, in the cytoprotective effect of exendin-4 against rapamycin-induced cell death.

JNK and p38 are involved in rapamycin-induced cell death in MIN6 cells

Previous studies found that rapamycin induces apoptosis in rh30, a human rhabdomyosarcoma cell line [14], and in islets isolated from *P. Obesus* [10], by activating JNK. In contrast, rapamycin inhibits palmitate-induced ER stress and apoptosis in INS-1E cells [15]. To clarify the involvement of JNK in rapamycin-induced cytotoxicity in MIN6 cells, 10 µM SP600125, a JNK inhibitor, was added into the media 30 min before treatment with 10 nM rapamycin for 12 h, when dead cells were counted by flowcytometer. SP600125 significantly inhibited rapamycin-induced cell death by 62.6 ± 9.1 % (◎ **Fig. 3a**). We also examined the involvement of p38, the other stress-activated protein kinase [16]. Ten µM SB203580, a p38 inhibitor, added to MIN6 cells 30 min before treatment with 10 nM rapamycin for 12 h resulted in significant inhibition of rapamycin-induced cell death by 36.8 ± 6.4 % (◎ **Fig. 3a**). These results indicate that rapamycin-induced cell death is mediated by JNK and p38 in MIN6 cells.

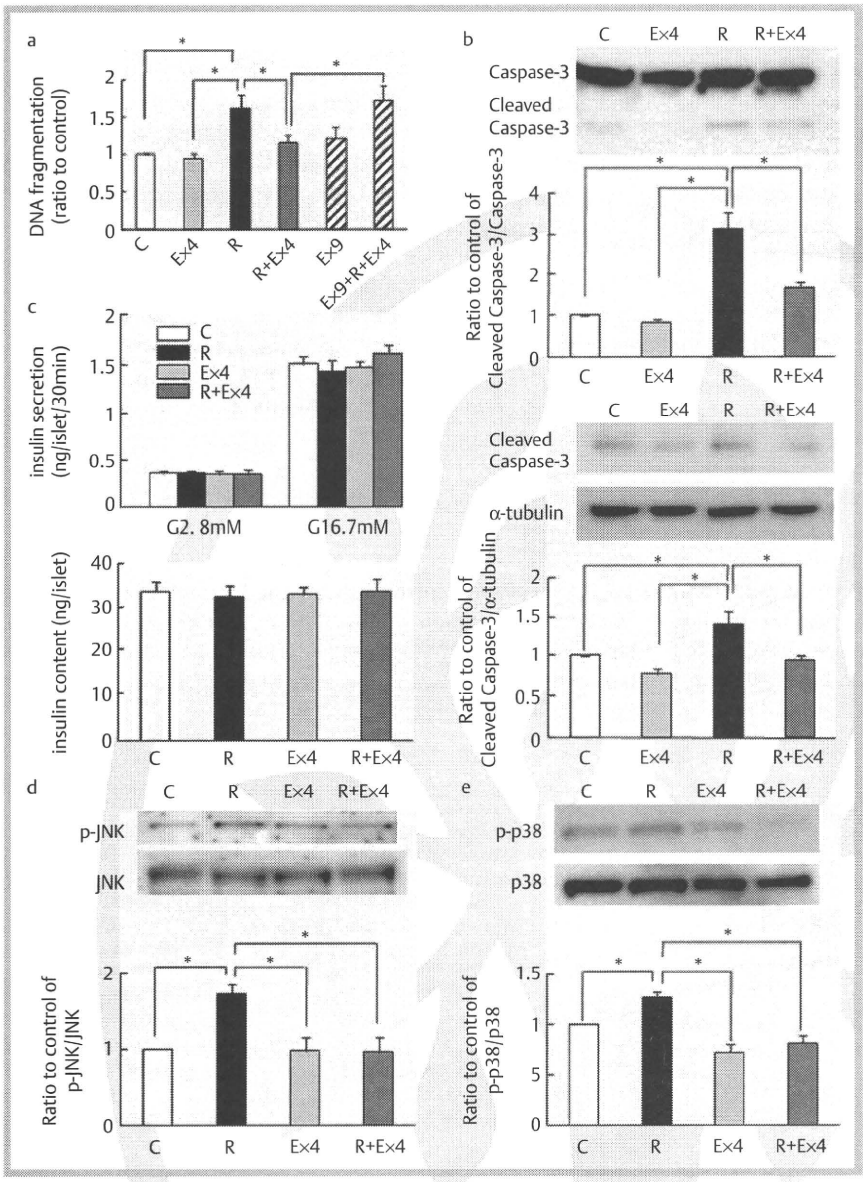

Fig. 4 Exendin-4 inhibits cell death and phosphorylation of JNK and p38 induced by rapamycin in Wistar rat primary islets. **a**: Primary islets were treated with 10 nM rapamycin and/or 10 nM exendin-4 and/or 100 nM exendin-9 for 12 h, and dead cells were detected by DNA fragmentation. Data are means ± SE of three independent experiments. * $p<0.05$ **b**: Western blot analysis of caspase-3 and cleaved caspase-3 in primary islets treated with 10 nM rapamycin and/or 10 nM exendin-4 for 12 h. Images are representative of three independent experiments. Graphs show relative ratio of cleaved caspase-3 v.s. caspase-3 or α-tubulin, respectively. * $p<0.05$. **c**: Glucose-stimulated insulin secretion and insulin content in Wistar rat islets treated with 10 nM rapamycin and/or 10 nM exendin-4 for 12 h. Data are means ± SE of three independent experiments. **d**, **e**: Primary islets were treated with 10 nM rapamycin and/or 10 nM exendin-4 for 30 min, and phosphorylation of JNK and p38 was detected by western blot. Images are representative of three independent experiments. Graphs show relative ratio of phosphorylated JNK or p38 vs. total JNK or p38, respectively, by treatment with rapamycin and/or exendin-4 compared to control (DMSO). Data are means ± SE of four independent experiments. * $p<0.05$. C: control (DMSO); R: rapamycin; Ex4: exendin-4; Ex9: exendin-9; G: glucose.

Exendin-4 inhibits phosphorylation of JNK and p38 induced by rapamycin

To confirm the involvement of JNK and p38 in rapamycin-induced cell death, MIN6 cells were incubated with 10 nM rapamycin for 30 min, and phosphorylation of JNK and p38 was detected by western blot analysis. Phosphorylation of JNK and p38 was significantly increased 2.9 ± 0.2-fold and 1.6 ± 0.3-fold, respectively, compared to that in nontreated cells (◎ **Fig. 3b** and **c**). In contrast, 10 nM exendin-4 decreased phosphorylation of both JNK and p38 in rapamycin-treated MIN6 cells (◎ **Fig. 3b** and **c**). However, rapamycin and exendin-4 were found not to affect phosphorylation of mitogen-activated protein kinase kinase (MKK) 3/6, a kinase of p38, or MKK4, a kinase of JNK (data not shown), indicating that dephosphorylation of both JNK and p38 by exendin-4 is not mediated by these upstream kinases.

PKA is involved in dephosphorylation of p38 by exendin-4

Because PKA partially inhibited rapamycin-induced cell death, we examined the effect of H89 on JNK and p38 phosphorylation. Fifteen μM H89 was added into the media of MIN6 cells 30 min before treatment with 10 nM rapamycin and/or 10 nM exendin-4 for 30 min, when phosphorylation of JNK and p38 was detected by western blot analysis. H89 did not affect decreased phosphorylation of JNK by exendin-4 (◎ **Fig. 3d**). By contrast, H89 significantly inhibited dephosphorylation of p38 by exendin-4 (◎ **Fig. 3e**), indicating that PKA regulates p38 phosphorylation.

Exendin-4 inhibits rapamycin-induced cell death and phosphorylation of JNK and p38 in Wistar rat islets

We lastly investigated whether exendin-4 inhibits cell death induced by rapamycin in primary islets by affecting phosphorylation of JNK or p38. Wistar rat islets were treated with 10 nM rapamycin and/or 10 nM exendin-4 for 12 h, and the number of dead cells was determined by DNA fragmentation. Rapamycin significantly increased DNA fragmentation by 1.6 ± 0.2-fold compared to that of control (DMSO) (◎ **Fig. 4a**), while exendin-4 significantly inhibited rapamycin-induced DNA fragmentation (◎ **Fig. 4a**). Exendin-9 again completely blocked the cytoprotective effect of exendin-4 (◎ **Fig. 4a**), indicating that such cytoprotective effect of exendin-4 is mediated by the GLP-1 receptor in primary islets. Caspase-3 activity also was significantly increased in rapamycin-treated islets, which was prevented by treatment with exendin-4 (◎ **Fig. 4b**). To determine whether the surviving

cells treated with exendin-4 were actually beta cells, islet beta cells were stained with Newport Green, a fluorescent indicator of zinc that allowed visualization of islet beta cells [17] after treatment with 10 nM rapamycin and/or 10 nM exendin-4 for 12 h. Fluorescence microscopy revealed Newport Green positive cells treated with rapamycin and exendin-4 that are almost the same as those treated with DMSO (control) or exendin-4 alone (data not shown). In addition, insulin content and glucose-stimulated insulin secretion (GSIS) were compared among rapamycin- and/or exendin-4-treated Wistar rat islets to determine whether or not these islets are still functional. After islets were incubated with 10 nM rapamycin and/or 10 nM exendin-4 for 12 h, the rapamycin and exendin-4 were washed out and the islets were then stimulated with 2.8 mM or 16.7 mM glucose for 30 min. The amounts of GSIS and insulin content were almost the same in rapamycin- and exendin-4-treated islets, indicating that islets treated with rapamycin and exendin-4 for 12 h are still functional (◉ **Fig. 4c**).

Finally, regulation of JNK and p38 by rapamycin or exendin-4 in primary islets was examined. Incubation with 10 nM rapamycin for 30 min significantly increased phosphorylation of JNK and p38 by 1.7±0.2-fold and 1.3±0.1-fold, respectively, which was reversed to control level by coincubation with exendin-4 (◉ **Fig. 4d** and **e**). These results indicate that exendin-4 protects primary islets from rapamycin-induced cytotoxicity by decreasing phosphorylation of JNK and p38.

Discussion

In the present study, we have demonstrated that rapamycin induces cytotoxicity in MIN6 cells and Wistar rat islets by phosphorylating JNK and p38, and that exendin-4 inhibits this effect by inhibiting phosphorylation of JNK and p38. This is the first report indicating that rapamycin and exendin-4 regulate phosphorylation not only of JNK but also of p38 in primary islets.

The molecular mechanism of the cytoprotective effect of exendin-4 is mediated by increased levels of cAMP that lead to activation of PKA, enhanced IRS-2 activity, and activation of Akt and ERK [7]. Our data also reveal that an increase in the cAMP concentration completely blocked rapamycin-induced cell death. However, LY294002 and PD98059 did not affect rapamycin-induced beta cell death, even though exendin-4 increased Akt and ERK phosphorylation. Phosphorylation of Akt and ERK also were not affected by treatment with rapamycin, suggesting that these kinases are not directly involved in the cytoprotective effect of exendin-4 on rapamycin-induced beta cell death.

On the other hand, exendin-4 and rapamycin both regulate phosphorylation of JNK and p38 in islet beta cells. Rapamycin increases JNK and p38 phosphorylation; exendin-4 decreases their phosphorylation. JNK and p38 are activated by cellular stress, and lead the cells to apoptosis [18]. In islet beta cells, phosphorylation of JNK and p38 are involved in cell death induced by IL-1β [19,20] and islet isolation [21,22]. Conversely, inhibition of JNK or p38 with specific inhibitors prevents cell death induced by islet isolation [22,23], indicating that JNK and p38 are significant molecules in pancreatic beta cell death. In addition, when Wistar rat islets were preincubated for 24 h, rapamycin decreased GSIS, most likely due to reduction in mitochondrial ATP production in the islets of these rats [24]. JNK and p38 are involved in beta-cell function, their activation also affecting insulin biosynthesis. JNK activates c-Jun, a downstream protein, and inhibits insulin gene transcription [25]. Furthermore, the p38 molecule is reported to repress rat insulin gene 1 promoter activated by GLP-1 [26]. Although insulin secretion and insulin content were not affected by pretreatment with 10 nM rapamycin and/or 10 nM exendin-4 for 12 h, inhibition of JNK and p38 activity by treatment with exendin-4 for a longer time may not only inhibit beta cell apoptosis but also increase insulin biosynthesis.

In summary, exendin-4 can inhibit rapamycin-induced beta cell death via a decrease in phosphorylation of both JNK and p38, and dephosphorylation of p38 by exendin-4 is accomplished at least partially through PKA signaling pathways. These results demonstrate that regulation of both JNK and p38 is important in the cytoprotective action of exendin-4 against rapamycin in pancreatic beta cells.

Acknowledgements

This study was supported by Scientific Research Grants from the Ministry of Education, Culture, Sports, Science, and Technology, Japan, and from the Ministry of Health, Labor, and Welfare, Japan, and also by Kyoto University Global COE Program "Center for Frontier Medicine".

Affiliations
[1] Department of Diabetes and Clinical Nutrition, Graduate School of Medicine, Kyoto University, Kyoto, Japan
[2] Japan Association for the Advancement of Medical Equipment, Tokyo, Japan
[3] Department of Endocrinology and Diabetes and Geriatric Medicine, Akita University School of Medicine, Akita, Japan
[4] Kansai Electric Power Hospital, Osaka, Japan
[5] CREST of Japan Science and Technology Cooperation (JST), Kyoto, Japan

References

1 *Kendall DM, Riddle MC, Rosenstock J, Zhuang D, Kim DD, Fineman MS, Baron AD.* Effects of exenatide (exendin-4) on glycemic control over 30 weeks in patients with type 2 diabetes treated with metformin and a sulfonylurea. Diabetes Care 2005; 28: 1083–1091
2 *Baggio LL, Drucker DJ.* Biology of incretins: GLP-1 and GIP. Gastroenterology 2007; 132: 2131–2157
3 *Li L, El-Kholy W, Rhodes CJ, Brubaker PL.* Glucagon-like peptide-1 protects beta cells from cytokine-induced apoptosis and necrosis: role of protein kinase B. Diabetologia 2005; 48: 1339–1349
4 *Yusta B, Baggio LL, Estall JL, Koehler JA, Holland DP, Li H, Pipeleers D, Ling Z, Drucker DJ.* GLP-1 receptor activation improves beta cell function and survival following induction of endoplasmic reticulum stress. Cell Metab 2006; 4: 391–406
5 *Wang Q, Brubaker PL.* Glucagon-like peptide-1 treatment delays the onset of diabetes in 8 week-old db/db mice. Diabetologia 2002; 45: 1263–1273
6 *Li Y, Hansotia T, Yusta B, Ris F, Halban PA, Drucker DJ.* Glucagon-like peptide-1 receptor signaling modulates beta cell apoptosis. J Biol Chem 2003; 278: 471–478
7 *Brubaker PL, Drucker DJ.* Minireview: Glucagon-like peptides regulate cell proliferation and apoptosis in the pancreas, gut, and central nervous system. Endocrinology 2004; 145: 2653–2659
8 *Tews D, Lehr S, Hartwig S, Osmers A, Paslack W, Eckel J.* Anti-apoptotic action of exendin-4 in INS-1 beta cells: comparative protein pattern analysis of isolated mitochondria. Horm Metab Res 2009; 41: 294–301
9 *Bell E, Cao X, Moibi JA, Greene SR, Young R, Trucco M, Gao Z, Matschinsky FM, Deng S, Markman JF, Naji A, Wolf BA.* Rapamycin has a deleterious effect on MIN-6 cells and rat and human islets. Diabetes 2003; 52: 2731–2739
10 *Fraenkel M, Ketzinel-Gilad M, Ariav Y, Pappo O, Karaca M, Castel J, Berthault MF, Magnan C, Cerasi E, Kaiser N, Leibowitz G.* mTOR inhibition by rapamycin prevents beta-cell adaptation to hyperglycemia and exacerbates the metabolic state in type 2 diabetes. Diabetes 2008; 57: 945–957

11 *Fujimoto S, Ishida H, Kato S, Okamoto Y, Tsuji K, Mizuno N, Ueda S, Mukai E, Seino Y.* The novel insulinotropic mechanism of pimobendan: Direct enhancement of the exocytotic process of insulin secretory granules by increased Ca2+ sensitivity in beta-cells. Endocrinology 1998; 139: 1133–1140
12 *Leist M, Gantner F, Bohlinger I, Germann PG, Tiegs G, Wendel A.* Murine hepatocyte apoptosis induced in vitro and in vivo by TNF-alpha requires transcriptional arrest. J Immunol 1994; 153: 1778–1788
13 *Webster AC, Lee VW, Chapman JR, Craig JC.* Target of rapamycin inhibitors (sirolimus and everolimus) for primary immunosuppression of kidney transplant recipients: a systematic review and meta-analysis of randomized trials. Transplantation 2006; 81: 1234–1248
14 *Huang S, Shu L, Dilling MB, Easton J, Harwood FC, Ichijo H, Houghton PJ.* Sustained activation of the JNK cascade and rapamycin-induced apoptosis are suppressed by p53/p21(Cip1). Mol Cell 2003; 11: 1491–1501
15 *Bachar E, Ariav Y, Ketzinel-Gilad M, Cerasi E, Kaiser N, Leibowitz G.* Glucose amplifies fatty acid-induced endoplasmic reticulum stress in pancreatic beta-cells via activation of mTORC1. PLoS One 2009; 4: e4954
16 *Rincón M, Davis RJ.* Regulation of the immune response by stress-activated protein kinases. Immunol Rev 2009; 228: 212–224
17 *Lukowiak B, Vandewalle B, Riachy R, Kerr-Conte J, Gmyr V, Belaich S, Lefebvre J, Pattou F.* Identification and purification of functional human beta-cells by a new specific zinc-fluorescent probe. J Histochem Cytochem 2001; 49: 519–528
18 *Mandrup-Poulsen T.* beta-cell apoptosis: stimuli and signaling. Diabetes 2001; 50 (Suppl 1): S58–S63
19 *Ammendrup A, Maillard A, Nielsen K, Aabenhus Andersen N, Serup P, Dragsbaek Madsen O, Mandrup-Poulsen T, Bonny C.* The c-Jun amino-terminal kinase pathway is preferentially activated by interleukin-1 and controls apoptosis in differentiating pancreatic beta-cells. Diabetes 2000; 49: 1468–1476
20 *Saldeen J, Lee JC, Welsh N.* Role of p38 mitogen-activated protein kinase (p38 MAPK) in cytokine-induced rat islet cell apoptosis. Biochem Pharmacol 2001; 61: 1561–1569
21 *Abdelli S, Ansite J, Roduit R, Borsello T, Matsumoto I, Sawada T, Allaman-Pillet N, Henry H, Beckmann JS, Hering BJ, Bonny C.* Intracellular stress signaling pathways activated during human islet preparation and following acute cytokine exposure. Diabetes 2004; 53: 2815–2823
22 *Ito T, Omori K, Rawson J, Todorov I, Asari S, Kuroda A, Shintaku J, Itakura S, Ferreri K, Kandeel F, Mullen Y.* Improvement of canine islet yield by donor pancreas infusion with a p38MAPK inhibitor. Transplantation 2008; 86: 321–329
23 *Noguchi H, Nakai Y, Matsumoto S, Kawaguchi M, Ueda M, Okitsu T, Iwanaga Y, Yonekawa Y, Nagata H, Minami K, Masui Y, Futaki S, Tanaka K.* Cell permeable peptide of JNK inhibitor prevents islet apoptosis immediately after isolation and improves islet graft function. Am J Transplant 2005; 5: 1848–1855
24 *Shimodahira M, Fujimoto S, Mukai E, Nakamura Y, Nishi Y, Sasaki M, Sato Y, Sato H, Hosokawa M, Nagashima K, Seino Y, Inagaki N.* Rapamycin impairs metabolism-secretion coupling in rat pancreatic islets by suppressing carbohydrate metabolism. J Endocrinol 2010; 204: 37–46
25 *Inagaki N, Maekawa T, Sudo T, Ishii S, Seino Y, Imura H.* c-Jun represses the human insulin promoter activity that depends on multiple cAMP response elements. Proc Natl Acad Sci USA 1992; 89: 1045–1049
26 *Kemp DM, Habener JF.* Insulinotropic hormone glucagon-like peptide 1 (GLP-1) activation of insulin gene promoter inhibited by p38 mitogen-activated protein kinase. Endocrinology 2001; 142: 1179–1187

The Journal of Nutrition
Nutrition and Disease

Dietary Fiber Intake Is Associated with Reduced Risk of Mortality from Cardiovascular Disease among Japanese Men and Women[1–3]

Ehab S. Eshak,[4] Hiroyasu Iso,[4]* Chigusa Date,[5] Shogo Kikuchi,[6] Yoshiyuki Watanabe,[7] Yasuhiko Wada,[8] Kenji Wakai,[9] Akiko Tamakoshi,[6] and the JACC Study Group[10]

[4]Public Health, Department of Social and Environmental Medicine, Osaka University Graduate School of Medicine, Yamadoka, 2-2 Suita-shi, Osaka, Japan 565-0871; [5]Department of Food Science and Nutrition, Faculty of Human Life and Environment, Nara Women's University, Kitauoya Nishimachi, Nara, Japan 630-8506; [6]Department of Public Health, Aichi Medical University School of Medicine, Nagakute, Aichi, Japan 480-1195; [7]Department of Epidemiology for Community Health and Medicine, Kyoto Prefectural University of Medicine Graduate School of Medical Sciences, Kajii-cho,Kawaramachi- Hirokoji, Kamigyo-ku, Kyoto, Japan 602-8566; [8]Department of Health Science, Faculty of Human Life and Environmental Science, Kochi Women's University, Eikokuji-cho, 5-15 Kochi-shi, Japan 780-8515; and [9]Department of Health and Community Medicine, Graduate School of Medicine, Nagoya University, 65 Tsurumai-cho, Shwa-Ku, Nagoya, Japan 466-8550

Abstract

Dietary fiber protects against coronary heart disease (CHD), but evidence in Asia is limited. We examined the association between dietary fiber intake and mortality from cardiovascular disease (CVD) in a Japanese population in a prospective study of 58,730 Japanese men and women aged 40–79 y in which dietary fiber intake was determined by a self-administered FFQ. The participants were followed up from 1988–1990 to the end of 2003. Hazard ratios (HR) and 95% CI of mortality were calculated per quintile of fiber intake. During the 14-y follow-up, a total of 2080 CVD deaths (983 strokes, 422 CHD, and 675 other CVD) were documented. Total, insoluble, and soluble dietary fiber intakes were inversely associated with risk of mortality from CHD and total CVD for both men and women. For men, the multivariable HR (95% CI) for CHD in the highest vs. the lowest quintiles were 0.81 [(95% CI, 0.61–1.09); P-trend = 0.02], 0.48 [(95% CI, 0.27–0.84); P-trend < 0.001], and 0.71 [(95% CI, 0.41–0.97); P-trend = 0.04] for total, insoluble, and soluble fiber, respectively. The respective HR (95% CI) for women were 0.80 [(95% CI, 0.57–0.97); P-trend = 0.01], 0.49 [(95% CI, 0.27–0.86); P-trend = 0.004], and 0.72 [(95% CI, 0.34–0.99); P-trend = 0.03], respectively. For fiber sources, intakes of fruit and cereal fibers but not vegetable fiber were inversely associated with risk of mortality from CHD. In conclusion, dietary intakes of fiber, both insoluble and soluble fibers, and especially fruit and cereal fibers, may reduce risk of mortality from CHD. J. Nutr. 140: 1445–1453, 2010.

Introduction

The WHO defines dietary fiber as the edible parts of plants or analogous carbohydrates that are resistant to digestion and absorption in human small intestine and undergoes complete or partial fermentation in large intestine (1). Burkitt and Trowell

[1] Supported by grants-in-aid for scientific research from the Ministry of Education, Science, Sports and Culture of Japan (Monbusho) (61010076, 62010074, 63010074, 1010068, 2151065, 3151064, 4151063, 5151069, 6279102, 11181101, 17015022, and 18014011) to the Japan Collaborative Cohort (JACC) Study.

[2] Author disclosures:-Eshak S. Ehab, Iso Hiroyasu, Date Chigusa, Kikuchi Shogo, Tamakoshi Akiko, Watanabe Yoshiyuki, Wada Yasuhiko, Wakai Kenji, and JACC Study Group, no conflict of interest.

[3] Supplemental Tables 1–3 are available with the online posting of this paper at jn.nutrition.org.

[10] The members of the JACC Study Group are as follows: Dr. Akiko Tamakoshi (present chairperson of the study group), Aichi Medical University School of Medicine; Mitsuru Mori and Fumio Sakauchi, Sapporo Medical University School of Medicine, Japan; Yutaka Motohashi, Akita University School of Medicine, Japan; Ichiro Tsuji, Tohoku University Graduate School of Medicine, Japan; Yosikazu Nakamura, Jichi Medical School, Japan; Hiroyasu Iso, Osaka University School of Medicine, Japan; Haruo Mikami, Chiba Cancer Center, Japan; Michiko Kurosawa, Juntendo University School of Medicine, Japan; Yoshiharu Hoshiyama, University of Human Arts and Sciences, Japan; Naohito Tamabe, Niigata University School of Medicine, Japan; Koji Tamakoshi, Nagoya University School of Medicine, Japan; Kenji Wakai, Nagoya University Graduate School of Medicine, Japan; Shinkan Tokudome, Nagoya City University Graduate School of Medical Sciences, Japan; Koji Suzuki, Fujita Health University School of Health Sciences, Japan, Shuji Hashimoto, Fujita Health University School of Medicine, Japan; Shogo Kikuchi, Aichi Medical University School of Medicine, Japan; Yasuhiko Wada, Kansai Rosai Hospital, Japan; Takashi Kawamura, Kyoto University Center for Student Health, Japan; Yoshiyuki Watanabe, Kyoto Prefectural University of Medicine Graduate School of Medical Science, Japan; Kotarou Ozasa, Hiroshima Laboratory, Radiation Effects Research Foundation; Tsuneharu Miki, Kyoto Prefectural University of Medicine Graduate School of Medical Science, Japan; Chigusa Date, Faculty of Human Environmental Sciences, Nara Women's University, Japan; Kiyomi Sakata, Iwate Medical University, Japan; Yoichi Kurozawa, Tottori University Faculty of Medicine, Japan; Takesumi Yoshimura, Fukuoka Institute of Health and Environmental Sciences, Japan; Yoshihisa Fujino, University of Occupational and Environmental Health, Japan; Akira Shibata, Kurume University School of Medicine, Japan; Naoyuki Okamoto, Kanagawa Cancer Center, Japan; Hideo Shio, Moriyama Municipal Hospital, Japan.

* To whom correspondence should be addressed. E-mail: fvgh5640@mb.infoweb.ne.jp or iso@pbhel.med.osaka-u.ac.jp.

Manuscript received February 8, 2010. Initial review completed March 18, 2010. Revision accepted May 24, 2010.
First published online June 23, 2010; doi:10.3945/jn.110.122358.

(2) stated that high dietary fiber intake may protect against chronic diseases; although their hypothesis initially focused on gastrointestinal diseases, it was later expanded to involve cardiovascular diseases (CVD).[11]

Reports of epidemiologic studies in Western countries have strongly suggested that dietary fiber intake offers protection against coronary heart disease (CHD) (3–9), but evidence has been limited in Asia. The mean daily Japanese dietary fiber intake was 20.5 g/d in 1952 and rapidly declined to ~70% of that level in 1970 (14.9 g/d), with little change thereafter (10,11). Meanwhile, during this period without declination of dietary fiber intake between 1970 and 1992, the age-adjusted mortality rates from CHD declined 50% for men and 65% for women (12) and have continued to decline (12,13). Nevertheless, the mean daily Japanese dietary fiber intake is similar to that of some Western countries (3,6) and lower than that of others (4,5,7–9). Therefore, it is worthwhile to investigate whether dietary fibers of different types and sources may protect against CHD with or without a threshold in a Japanese population.

Participants and Methods

Study population. The Japan Collaborative Cohort Study for Evaluation of Cancer Risks, a large prospective study sponsored by the Ministry of Education, Sports and Science, was carried out between 1988 and 1990 and covered a total of 110,792 participants (46,465 male and 64,327 female) aged 40–79 y. Participants were enrolled from 45 study areas throughout Japan, mostly from the general population or those who had undergone municipal health check-ups and completed self-administered questionnaires covering lifestyle data and medical histories of previous CVD and cancer at baseline. A subsample of 39,393 cohort participants donated a residual serum sample that was partitioned into 0.3–0.5-mL aliquots and stored at −80 C° until laboratory analysis. The details of the study procedure were described elsewhere (14,15). In most communities, informed consent was obtained from each participant, except in a few study areas where informed consent was obtained at the community level after the purpose of the study and confidentiality of the data had been explained to community leaders. The ethics committees of the Nagoya University School of Medicine and Osaka University approved the protocol of this investigation.

We excluded 16,109 participants (4683 men and 11,426 women) with a medical history of cancer, stroke, or CHD, and 123 with energy intakes above or below plausible intakes (<500 or >3500 kcal/d = <2096 kJ/d or >14,645 kJ/d). Also, participants whose responses to the FFQ were insufficient, which means failure to give an answer to 5 or more items of the 40 food items of the FFQ, and/or no answer for current rice intake, and/or no answer for current miso soup intake, and/or no answer for current alcohol consumption were excluded. A total of 58,730 (23,119 men and 35,611 women) were eligible for the study.

Mortality surveillance. For mortality surveillance in each of the communities, investigators conducted a systematic review of death certificates, all of which had been forwarded to the public health center in the area of residency. Mortality data were then centralized at the Ministry of Health and Welfare and the underlying causes of death were coded according to the National Vital Statistics system, which is based on the International Classification of Diseases, 10th revised edition.

Participants who died after they had moved from their original communities were treated as censored cases. Of the total 58,730 participants, 2487 (4.2%) moved. Cause-specific mortality was categorized as stroke (I60–I69), CHD (I20–I25), other CVD (I30–I52), and total CVD (I01–I99). The follow-up of mortality was conducted until the end of 2003, except for 4 communities, where follow-up was terminated at the end of 1999.

Diet and baseline survey. A self-administered questionnaire, which included a FFQ, was used to collect the baseline data for demographic characteristics; history of hypertension, diabetes mellitus, and other chronic diseases; family history of cancer; and height and weight, as well as habits related to smoking, alcohol consumption, exercise, and diet.

The FFQ representing the dietary component of the survey included 40 food items (15). Participants were asked about average intake frequency without specifying portion size. There were 5 response choices: almost never, once or twice/mo, once or twice/wk, 3–4 times/wk, and almost every day. Food and nutrient intakes were computed using the Japanese food composition table (4th revised edition) (16) and standard portion sizes derived from weighted dietary records (DR). The details of the study procedure were described elsewhere (14,15). Key's score was calculated using this formula: Key's score = 1.35 [2energy from SFA (% energy) − energy from PUFA (% energy)] + 1.52 [cholesterol intake (mg/1000kcal)][2] (17). Values for total dietary fiber (TDF), insoluble dietary fiber (IDF), and soluble dietary fiber (SDF), obtained by enzymatic-gravimetric methods by Prosky et al. (18), and were derived from the food composition table. The FFQ was validated by using 4 3-d weighed DR over a 1-y period as a reference standard (19). The authors reanalyzed data from the validation study to take into account skewed distributions of nutrient intakes and within-person variations for intake (20). The deattenuated correlation coefficients for energy-adjusted intakes between the FFQ and DR were 0.46 for TDF, 0.47 for IDF, 0.42 for SDF, 0.30 for cereal fiber, 0.33 for fruit fiber, and 0.41 for vegetable fiber ($P < 0.001$ for all). The ratios of mean intakes estimated by the FFQ to those calculated from the DR were 0.60, 0.58, 0.51, 0.66, 0.84, and 0.53 for total, insoluble, soluble, cereal, fruit, and vegetable fibers, respectively.

Statistical analysis. Total, insoluble, soluble, cereal, fruit, and vegetable dietary fiber intakes were calorie adjusted by using the residual method (21) and modeled as categorical (5 quintile groups) variables in the primary analysis. Statistical analyses were based on sex-specific mortality rates of disease outcomes during the follow-up period from 1988–1990 to 2003 (until 1999 for 4 areas). The person-years of the follow-up were calculated from the date of completing the baseline questionnaire to death, moving out of the community, or the end of follow-up, whichever came first.

Because most of distributions for the dietary variables are skewed, sex-specific medians with interquartile range or proportions of cardiovascular risk factors were calculated. The sex-specific hazard ratios (HR) with 95% CI for mortality by disease outcome (stroke, CHD, other CVD, and total CVD) were calculated with reference to the risk according to energy-adjusted total, insoluble, soluble, and different sources of fiber intakes. For Cox proportional hazard models, the PHREG procedure of SAS/STAT software (version 9.1; SAS Institute) was used. There was no evidence that proportional hazards assumptions were violated, as indicated by the lack of significant interaction between the predictors and a function of survival time in the model. The estimates were presented as age-adjusted and multivariable-adjusted models including other potential confounding factors: history of hypertension, history of diabetes, BMI (sex-specific quintiles), smoking status (never, ex-smoker, current smoker of 1–19, and ≥20 cigarettes/d), alcohol consumption (nondrinker, ex-drinker, current drinker of 0.1–22.9, 23.0–45.9, 46.0–68.9, and ≥69.0 g ethanol/d), hours of exercise (almost never, 1–2, 3–4 and ≥5 h/wk), hours of walking (almost never, 0.5, 0.6–0.9, and ≥1 h/d), perceived mental stress (low, moderate, and high), education level (primary school, junior high school, high school, and college or higher), sleep duration (≤6 h, 6–<7 h, 7–<8 h, 8–>9 h, ≥9 h/d), fish, sodium, SFA, (n-3) fatty acids, folic acid, and vitamin E intakes (sex-specific energy-adjusted quintiles), and total energy intake. Because of the high correlations between soluble and insoluble fibers ($r = 0.96$ for men and 0.95 women), they could not be distinguished in the multivariate analysis

Because of low to moderate correlations between different sources of fibers (cereal, fruit, and vegetables), a 3rd model was added for each with further adjustment for intakes of other sources of fiber: for men, r = −0.31 between cereal and fruit fibers, −0.43 between cereal and

[11] Abbreviations used: CHD, coronary heart disease; CVD, cardiovascular disease; DR, dietary record; HR, hazard ratio; IDF, insoluble dietary fiber; SDF, soluble dietary fiber; TDF, total dietary fiber.

vegetable fibers, and 0.29 between fruit and vegetable fibers, and for women, $r = -0.33$ between cereal and fruit fibers, −0.43 between cereal and vegetable fibers, and 0.20 between fruit and vegetable fibers. For tests for linear trends across increasing categories of fiber, the categories were treated as a continuous variable and the median intake for the category was designated as its value. All statistical testing were 2-sided, and for all tests $P < 0.05$ was considered significant.

Results

Among the 58,730 adults aged 40–79 y at baseline examination, 2080 total CVD deaths were recorded during the 14.3 y of follow-up, comprising 983 deaths from stroke, 422 from CHD, and 675 from other CVD.

At baseline, both men and women with higher TDF intake were ~6–9 y older, with higher BMI, more educated, more likely to practice sports and to walk, less likely to drink, less likely to be current smokers, and less likely to have a history of hypertension. Furthermore, higher TDF intake was positively associated with higher intakes of fish, vegetables, fruit, meat, milk/dairy, soy, calcium sodium, potassium, vitamin B-6, isoflavones, (n-3) fatty acids, SFA, monounsaturated fatty acid, and PUFA, dietary cholesterol, and the Key's score (Table 1).

As for the serum chemistry in the subsample of men ($n = 6767$) and women ($n = 13,102$), higher TDF intake was inversely associated with serum total cholesterol and triglycerides. Similar trends were observed for SDF and IDF (results not shown). There was an ~0.8- to 1.1-fold greater median TDF intake in the highest compared with the lowest quintiles of TDF for men and women.

Sex-specific, age-adjusted mortality from CVD and total CVD was lower for both men and women with higher TDF intake. After adjustment for cardiovascular risk factors and fish, sodium, SFA, (n-3) fatty acid, folate, vitamin E, and total energy intakes, this tendency toward lower mortality was slightly attenuated but remained significant. The multivariable HR of CHD in the highest compared with lowest quintiles were 0.81 [(95% CI, 0.61–1.09); P-trend = 0.02] for men, 0.80 [(95% CI, 0.57–0.97); P-trend = 0.01] for women, and 0.79 [(95% CI, 0.61–0.98); P-trend = 0.01] overall when men and women were combined adjusting for sex (**Supplemental Table 1**). The multivariable HR of total CVD in the highest compared with lowest quintiles were 0.83 [(95% CI, 0.63–1.09); P-trend = 0.05] for men, 0.82 [(95% CI, 0.57–0.97); P-trend = 0.04] for women, and 0.82 [(95% CI, 0.60–0.99); P-trend = 0.02] overall (Supplemental Table 1). There were no significant associations of TDF intake with risk of mortality from stroke or other CVD for either sex (Table 2).

After dividing TDF into IDF and SDF, the age-adjusted risks of mortality from CHD and total CVD were lower for both men and women with higher IDF intake (**Table 3**). After adjustment for cardiovascular risk factors and dietary variables, the multivariable HR for mortality from CHD in the highest compared with lowest quintiles of IDF intake were 0.48 [(95% CI, 0.27–0.84); P-trend < 0.001] for men, 0.49 [(95% CI, 0.27–0.86); P-trend = 0.004] for women, and 0.46 [(95% CI, 0.30–0.85); P-trend = <0.001] overall (**Supplemental Table 2**). For mortality from total CVD, the multivariable HR were 0.82 [(95% CI, 0.65–0.98); P-trend = 0.04] for men, 0.69 [(95% CI, 0.53–0.91); P-trend = 0.02] for women, and 0.77 [(95% CI, 0.61–0.96); P-trend = 0.01] overall (Supplemental Table 2). There were no significant associations of IDF intake with risk of mortality from stroke or other CVD for either sex.

Age-adjusted mortality from CHD and total CVD were lower for both men and women with higher SDF intake. The multivariable HR of mortality from CHD in the highest compared with lowest quintiles of SDF intake were 0.71 (0.41–0.97; P-trend = 0.04) for men, 0.72 [(0.34–0.99) P-trend = 0.03] for women, and 0.69 [(0.44–0.94) P-trend = 0.01] overall (Supplemental Table 2). For mortality from total CVD, the multivariable HR were 0.81 [(95% CI, 0.63–1.04); P-trend = 0.04] for men, 0.83 [(95% CI, 0.53–1.02); P-trend = 0.04] for women, and 0.80 [(95% CI, 0.60–0.99); P-trend = 0.02] overall (Supplemental Table 2). There were no significant associations of SDF intake with risk of mortality from stroke or other CVD for either sex.

We analyzed separately the effects of 3 main food sources of dietary fiber (**Table 4; Supplemental Table 3**). Fruit fiber intake was significantly inversely associated with risk of mortality from CHD. The multivariable HR for CHD after further adjusting for other sources of fiber were 0.55 [(95% CI, 0.32–0.96); P-trend = 0.03] for men and 0.42 [(95% CI, 0.33–0.81); P-trend = 0.01] for women. Cereal fiber intake was inversely associated with risk of mortality from CHD; the multivariable HR were 0.89 [(95% CI, 0.65–1.01); P-trend = 0.06] for men and 0.79 [(95% CI, 0.59–0.97); P-trend = 0.04) for women. There was no significant association of vegetable fiber intake with risk of mortality from CHD for either sex.

Discussion

This 14-y prospective study of Japanese men and women aged 40–79 y showed inverse relationships of total, insoluble, soluble, cereal, and fruit fiber intakes and risk of mortality from CHD. These inverse associations were similar for both men and women and stronger for IDF than SDF and for fruit than for cereal fibers.

The inverse associations with mortality from CHD were observed for both IDF and SDF intakes in a pooled analysis of 10 American and European cohort studies (7); HR per 10-g/d increment were 0.80 (95% CI, 0.69–0.92) for IDF and 0.72 (95% CI, 0.55–0.93) for SDF intakes. Further, the somewhat stronger association for IDF than SDF in the present study is consistent with the results of the Health Professionals Follow-up Study (9) and the Iowa Women's Health Study (22). In the Health Professionals Follow-up Study, the multivariable HR of mortality from CHD for each 10-g increment of IDF intake was 0.75 (95% CI, 0.59–0.94) and that of SDF was 1.07 (95% CI, 0.57–2.02). In the Iowa Women's Health Study, the multivariable HR of mortality from CHD in the highest compared with the lowest quintiles was 0.70 [(95% CI, 0.50–0.96); P-trend = 0.05] for IDF and 0.79 [(95% CI, 0.58–1.08); P-trend = 0.30] for SDF.

The inverse associations of fruit and cereal fiber intakes, but not vegetable fiber intake, with mortality from CHD in the present study were consistent with findings from previous studies: the Women's Health study (23), Nurse Health study (24), Cardiovascular Health Study (25), and the pooled analysis of 10 American and European cohort studies (7).

The inverse association between dietary fiber and CHD can be explained by different mechanisms, such as improving blood lipid profile through its cholesterol-lowering effect (26), lowering blood pressure (27) via reduction of abdominal obesity and improvement of vascular reactivity (28), improving insulin sensitivity (29), inhibiting a postprandial rise of glucose and triglycerides (30), and improving fibrinolytic activity (31,32), all of which may prevent or delay the development of atherosclerosis. Previous studies suggested that those effects were derived by both IDF and SDF (7–9,31,33). However, SDF may have a stronger cholesterol-lowering effect (26), whereas IDF may have a stronger clotting factor reduction effect (23,31).

TABLE 1 Cardiovascular risk factors in Japanese men and women according to quintiles of TDF intake at the baseline examination[1]

	Men					Women				
	Q1 (low)	Q2	Q3	Q4	Q5 (high)	Q1 (low)	Q2	Q3	Q4	Q5 (high)
Median intake, *g/d*	6.8	8.7	10.2	11.7	14.0	7.4	9.2	10.50	11.9	13.8
Participants at risk, *n*	4623	4624	4624	4624	4624	7122	7122	7122	7122	7122
Age, *y*	52 (45–60)	55 (47–62)	55 (47–63)	58 (49–64)	60 (52–66)	53 (46–61)	55 (47–62)	56 (48–63)	57 (49–64)	59 (52–66)
BMI, *kg/m²*	22.5 (20.8–24.5)	22.5 (20.8–24.3)	22.6 (20.8–24.4)	22.6 (20.8–24.5)	22.6 (20.8–24.6)	22.7 (20.8–24.8)	22.6 (20.8–24.6)	22.7 (20.8–24.7)	22.8 (20.9–24.8)	22.8 (21.0–24.9)
History of hypertension, %	20	21	20	18	16	18	20	20	21	22
History of diabetes, %	6	6	7	5	6	3	4	3	3	3
Ethanol intake, *g/d*	46 (23–57)	34 (23–46)	23 (17–46)	23 (11–46)	23 (11–46)	7 (3–23)	5 (2–11)	5 (2–11)	5 (2–11)	5 (2–11)
Current smoker, %	62	55	53	52	48	8	6	4	4	3
College or higher education, %	17	18	19	20	19	9	10	11	12	12
High perceived mental stress, %	25	25	25	24	23	23	21	21	20	19
Exercise ≥5h/wk, %	26	30	32	33	35	20	21	23	26	26
Walking ≥1h/d, %	67	67	69	72	73	70	70	72	74	75
Time sleeping, *h*	7.0 (7.0–8.0)	7.0 (7.0–8.0)	7.0 (7.0–8.0)	7.7 (7.0–8.0)	8.0 (7.0–8.0)	7.0 (6.0–8.0)	7.0 (6.0–8.0)	7.0 (6.0–8.0)	7.0 (6.5–8.0)	7.0 (6.5–8.0)
Food group intakes,[2] *g/d*										
Fish	35 (22–56)	39 (25–60)	43 (26–70)	45 (30–72)	57 (38–84)	38 (22–56)	40 (25–62)	43 (27–69)	48 (31–72)	56 (36–80)
Vegetables	45 (29–66)	63 (43–94)	80 (52–118)	105 (73–730)	744 (117–812)	57 (37–85)	80 (52–118)	99 (69–714)	131 (89–772)	779 (136–824)
Fruit	34 (8–54)	50 (23–80)	61 (34–107)	80 (39–127)	114 (80–161)	54 (23–88)	80 (39–114)	96 (61–127)	114 (80–161)	127 (96–161)
Meat	22 (12–32)	23 (14–35)	25 (14–36)	27 (16–39)	29 (18–43)	26 (14–38)	26 (16–38)	26 (16–39)	27 (16–39)	27 (15–41)
Milk and dairy products	37 (7–146)	73 (7–146)	73 (7–147)	79 (13–147)	97 (17–147)	78 (8–147)	81 (21–151)	106 (31–151)	146 (31–152)	123 (31–152)
Soy	15 (13–32)	30 (15–39)	32 (15–60)	39 (21–629	60 (32–69)	21 (15–32)	32 (15–50)	32 (21–62)	39 (32–62)	62 (39–70)
Selected nutrient intakes[2]										
Vitamin B-6, *mg/d*	0.8 (0.6–1.0)	0.9 (0.7–1.1)	1.0 (0.8–1.2)	1.1 (0.9–1.3)	1.3 (1.1–1.5)	0.8 (0.7–1.0)	0.9 (0.8–1.1)	1.0 (0.9–1.2)	1.1 (1.0–1.3)	1.3 (1.1–1.5)
(n-3) Fatty acids, *mg/d*	1.1 (0.8–1.5)	1.3 (1.0–1.8)	1.5 (1.2–2.0)	1.7 (1.4–2.2)	2.1 (1.7–2.6)	1.2 (0.9–1.6)	1.4 (0.8–1.8)	1.5 (1.2–2.0)	1.7 (1.4–2.2)	2.1 (1.6–2.6)
Calcium, *mg/d*	273 (270–493)	440 (330–551)	492 (370–606)	554 (429–660)	634 (514–747)	415 (297–527)	470 (343–583)	518 (366–624)	566 (437–670)	626 (494–739)
Potassium, *mg/d*	1736 (1394–2096)	2004 (1651–2371)	2229 (1872–2626)	2525 (2154–2911)	3008 (2614–3450)	1879 (1519–2246)	2114 (1763–2482)	2333 (1962–2700)	2590 (2236–2949)	2995 (2603–3391)
Sodium, *mg/d*	1319 (965–1772)	1778 (1312–2318)	2167 (1675–3140)	2498 (2006–2965)	2954 (2475–3485)	1335 (1001–1772)	1675 (1262–2168)	1997 (1535–2474)	2315 (1827–2778)	2731 (2246–3218)
Isoflavones, *mg/d*	12 (7–24)	25 (12–38)	34 (19–42)	39 (28–46)	46 (38–51)	12 (7–19)	19 (12–33)	28 (17–40)	37 (24–44)	44 (34–51)
SFA, *g/d*	8 (6–10)	9 (6–11)	9 (7–12)	10 (8–12)	11 (8–13)	9 (6–11)	9 (7–12)	10 (7–12)	10 (8–12)	11 (8–13)
Monounsaturated fatty acids, *g/d*	8 (6–10)	9 (7–11)	9 (7–12)	10 (8–12)	12 (9–14)	9 (6–11)	9 (7–11)	10 (8–12)	10 (8–12)	11 (9–14)
PUFA, *g/d*	5 (4–6)	6 (5–7)	7 (6–8)	8 (6–9)	9 (8–11)	5 (4–7)	6 (5–7)	7 (5–8)	7 (6–9)	9 (7–10)
Cholesterol, *g/d*	213 (142–316)	240 (161–332)	263 (183–349)	297 (205–367)	339 (236–401)	220 (148–323)	238 (166–336)	261 (183–349)	287 (199–365)	318 (218–390)
Energy, *kJ/d*	7457 (6046–8838)	7000 (5640–8499)	6950 (5585–8503)	7013 (5740–8520)	7281 (6125–8851)	6021 (5007–7365)	5648 (4794–6590)	5748 (4911–6590)	5954 (5120–6757)	6259 (5313–7155)
Keys score,[3] *mmol/L*	0.62 (0.51–0.74)	0.67 (0.56–0.80)	0.69 (0.57–0.82)	0.72 (0.61–0.84)	0.74 (0.62–0.86)	0.74 (0.60–0.88)	0.80 (0.67–0.93)	0.81 (0.69–0.93)	0.82 (0.69–0.93)	0.82 (0.69–0.92)
Serum chemistry of subsample, *n* = 19,869										
Participants at risk, *n*	1403	1383	1378	1317	1286	2964	2807	2571	2434	2326
Total cholesterol, *mmol/L*	4.9 (4.3–5.5)	4.8 (4.3–5.5)	4.9 (4.3–5.5)	4.8 (4.2–5.4)	4.8 (4.3–5.4)	5.2 (4.6–5.8)	5.2 (4.6–5.9)	5.2 (4.6–5.9)	5.2 (4.7–5.8)	5.1 (4.5–5.7)
HDL-cholesterol, *mmol/L*	1.3 (1.1–1.6)	1.3 (1.1–1.6)	1.3 (1.1–1.6)	1.3 (1.1–1.5)	1.3 (1.1–1.6)	1.4 (1.2–1.6)	1.4 (1.2–1.7)	1.4 (1.2–1.6)	1.4 (1.2–1.6)	1.4 (1.2–1.6)
Triglycerides, *mmol/L*	1.3 (0.87–1.9)	1.2 (0.87–1.8)	1.3 (0.87–1.8)	1.2 (0.88–1.7)	1.2 (0.88–1.7)	1.2 (0.83–1.6)	1.1 (0.77–1.5)	1.1 (0.84–1.6)	1.1 (0.77–1.5)	1.1 (0.77–1.5)

[1] Values are median (interquartile range), or percentages.
[2] Food and nutrient intakes were energy-adjusted using the residual method.
[3] Keys score was calculated by this formula: Keys score = 1.3542 [energy from SFA (% energy)] − [energy from PUFA (% energy)] + 1.52 [cholesterol intake (mg/1000 kcal)]².

TABLE 2 Sex-specific HR and 95% CI for mortality from CVD according to quintiles of TDF intake

	Men						Women					
	Q1 (Low)	Q2	Q3	Q4	Q5 (High)	*P*-trend[1]	Q1 (Low)	Q2	Q3	Q4	Q5 (High)	*P*-trend[1]
n	4623	4624	4624	4624	4624		7122	7122	7122	7122	7122	
Range, *g/d*	<7.8	7.8–9.4	9.5–10.8	10.9–12.6	>12.6		<8.5	8.5–9.9	10.0–11.1	11.2–12.7	>12.7	
Person-years	57,080	57,426	57,863	57,901	58,247		89,055	89,450	90,951	91953	93241	
Total stroke												
Cases, *n*	60	149	119	91	80		71	67	102	128	116	
Age-adjusted HR (95%CI)	1	1.32 (0.94–1.70)	1.37 (0.96–1.77)	1.33 (0.93–1.70)	1.03 (0.78–1.37)	0.642	1	0.97 (0.78–1.21)	1.01 (0.82–1.24)	1.13 (0.92-1.38)	1.19 (0.97-1.45)	0.364
Multivariable HR (95%CI)[2]	1	1.14 (0.74–1.76)	1.12 (0.74–1.69)	1.15 (0.70–1.56)	1.09 (0.75–1.58)	0.555	1	0.78 (0.55–1.12)	1.08 (0.76–1.54)	0.89 (0.61-1.30)	1.05 (0.73-1.51)	0.775
CHD												
Cases, *n*	40	60	50	41	40		38	35	41	47	30	
Age-adjusted HR (95%CI)	1	0.83 (0.62–1.11)	0.70 (0.52–0.93)	0.60 (0.44–0.82)	0.77 (0.58–1.03)	0.013	1	1.04 (0.74–1.47)	0.85 (0.59–1.14)	0.79 (0.54-0.98)	0.79 (0.54-0.96)	0.021
Multivariable HR (95%CI)[2]	1	0.83 (0.62–1.12)	0.69 (0.51–0.93)	0.59 (0.43–0.81)	0.81 (0.61–1.09)	0.022	1	1.03 (0.76–1.48)	0.86 (0.61–1.13)	0.81 (0.52-0.99)	0.80 (0.57-0.97)	0. 014
Other CVD												
Cases, *n*	45	94	75	64	55		52	51	78	86	75	
Age-adjusted HR (95%CI)	1	1.35 (0.93–1.97)	1.05 (0.74–1.51)	1.07 (0.62–1.34)	0.99 (0.68–1.45)	0.464	1	1.13 (0.86–1.49)	0.99 (0.60–1.41)	0.87 (0.59-1.29)	1.11 (0.86-1.44)	0.254
Multivariable HR (95%CI)[2]	1	1.25 (0.87–1.79)	0.92 (0.65–1.32)	1.06 (0.62–1.36)	0.78 (0.54–1.13)	0.313	1	1.18 (0.91–1.54)	0.97 (0.74–1.26)	0.78 (0.55-1.10)	1.06 (0.74-1.51)	0.212
Total CVD												
Cases, *n*	145	303	244	196	175		161	153	221	261	221	
Age-adjusted HR(95%CI)	1	1.02 (0.88–1.17)	0.91 (0.79–1.05)	0.84 (0.52–1.08)	0.84 (0.66–1.02)	0.043	1	1.17 (0.89–1.39)	1.10 (0.86–1.26)	0.84 (0.68-1.04)	0.81 (0.57-0.98)	0.061
Multivariable HR (95%CI)[2]	1	1.06 (0.92–1.22)	0.92 (0.80–1.06)	0.86 (0.55–1.15)	0.83 (0.63–1.09)	0.054	1	1.21 (0.94–1.44)	1.06 (0.82–1.19)	0.95 (0.69-0.99)	0.82 (0.57-0.97)	0.044

[1] Based on tests for trend across quintiles of fiber intake by assigning the median value of each quintile.

[2] Cox proportional hazard model adjusted for age, BMI, history of hypertension, history of diabetes, alcohol consumption, smoking, education level, hours of exercise, hours of walking, perceived mental stress, sleep fish, SFA, (n-3) fatty acids, sodium, folate, and vitamin E.